Ecomorphodynamics of the Avon River Upstream of the Windsor Causeway During Modified Gate Operations – Summer 2022

Prepared for:

Nova Scotia Department of Public Works

Prepared by:

CBWES Inc.

October 2023

Publication No. 80

<Page left intentionally blank>

TABLE OF CONTENTS

LIST OF FIGURES

LIST OF TABLES

ACKNOWLEDGEMENTS & DISCLAIMER

Financial support for this project was provided by the Nova Scotia Department of Public Works (NSDPW). Previous funding from NS Department of Transportation and Infrastructure Renewal, NS Department of Agriculture, Land Protection Section and Natural Resources Canada permitted the historical analysis used within this report. In addition, we acknowledge the Canadian Foundation for Innovation for infrastructure funding of equipment essential for this analysis. We would like to acknowledge and thank Tim Webster from the Advanced Geomatics Research group at the Center for Geographic Sciences for flying and processing the original 2007 lidar aerial survey.

Technical/Field Support: Emily Baker, Kayla Williams, Kailey Nichols, Makadunyiswe Ngulube, Greg Baker, Leah Rudderham, Macy Giles, Darren Porter and crew.

Authors: Jocelyn Kickbush, Jennie Graham, Tony Bowron, Danika van Proosdij, Sam Lewis, Kirsten Ellis

***Recommended Citation*:** Kickbush, J., Graham, J., Bowron, T.M., van Proosdij, D., Lewis, S., Ellis, K. 2022. Ecomorphodynamics of the Avon River Upstream of the Windsor Causeway During Modified Gate Operations – Summer 2022. Prepared for Nova Scotia Department of Public Works. CBWES Publication No. 86. Halifax, NS.

Disclaimer:

EXECUTIVE SUMMARY

The Avon River and corresponding estuary is a dynamic, coastal system that has a long history of morphodynamic change in response to natural and anthropogenic driving forces. The construction of the Avon River causeway and tide gate (1968–1970) significantly affected the hydrodynamics and sediment transport processes at play in the system. This change in processes resulted in the rapid accumulation of fine sediments (1970s and '80s) downstream of the tide gate and the creation of a freshwater reservoir upstream of the tide gate. However, recent changes in the frequency of gate opening to allow fish passage and construction activities on the Windsor Marsh have resulted in substantial changes in the ecological conditions upstream of the causeway. Between 2016 and March 2021 the frequency of gate openings and tidal waters flowing upstream for short durations increased due to ongoing gate manipulations (Graeme Matheson, NSDA, personal communication, 28 February 2022). On 19 March 2021, a Ministerial order was issued by DFO Minister Bernadette Jordan dictating that the gates must be fully open during outgoing tides and for a minimum of 10 minutes on the incoming tides to allow salt water upstream, which has further impacted the ecomorphodynamics of the system. This report documents habitat conditions upstream of the Avon River Causeway in the summer of 2022, following the second year of Phase 1 upgrades to the causeway as part of the Highway 101 Twinning Project and modified operations of the gate.

Geospatial

Aerial photography, Digital Surface Model (DSM) and elevation transects show that the study area is characterized by a narrow river channel and a wide, relatively flat floodplain (former riverbed/tidal mud flat). The floodplain, whose upland boundaries are the historic banks of the Avon River, widens as one moves downstream from Sangster's Bridge to the Windsor Causeway. The morphology is typical for tidal rivers in the Bay of Fundy. Comparing the 2022 DSM to the 2022 GNSS points (ground surface elevations) shows that the flood plain was heavily vegetated in September 2022. When surveyed points were compared to the corresponding DSM elevation, there was found to be a mean difference of 32 cm ± 31 cm. While the tallest vegetation was found on Transect 2, mean vegetation height is greatest along transects T7 and T8, furthest away from tidal influence and at higher elevations than transects lower in the estuary. Vegetation and Sediment Station elevations range between -1.156 m and 4.198 m CGVD2013, with a mean elevation of 0.718 ± 1.014 m.

Hydrology

Water levels recorded downstream (located within the aboiteau culvert and immediately downstream from Gate 1) and 600 m upstream of the Avon River Causeway (mounted on the underside of Trunk 1 Bridge) were obtained from the Nova Scotia Department of Agriculture (NSDA) for the period of January to December 2022. The highest tide of the year upstream of the aboiteau structure was 3.1 m CGVD2013 on 18 February 2022, and was due to the upstream spilling of hydroelectric dam that coincided with a storm event with 27.8 mm of total precipitation. This tide event was five times higher than the average high water level elevation which was -0.57 ± 0.54 m and did not coincide with the highest tide event downstream which occurred on 2 January 2022.

Vegetation and Habitat

Vegetation surveys found species from a variety of habitats: wet meadow, freshwater marsh, salt marsh and a handful of weedy (ruderal or first colonizer) species. There were many plots, especially at lower elevations, with high scores for wetland indicator status. The lowest scores were still in the facultative wetland category, indicating that plants with an affinity for wet sites are dominant here. Halophytes were abundant within the study area, with an average of 23% coverage across all plots. Freshwater and salt-tolerant wetland species coexisted in the same plots indicating that typical salt marsh zonation has yet to occur. Bare ground comprised only 13% of the classified area which demonstrates the rapid colonization following the enforcement of the ministerial order. A gradient was observed along the river with distance from the tide gate—with dominant species transitioning from saltwater (T1 and 2, 50 m from causeway) to brackish and freshwater species (T3 and 8, 1.5 to 6 km from causeway). Wetland scores decreased as elevation increased until Transects 7 and 8 (6 km from causeway) where wetland scores were higher despite higher elevations. This may point to changes in hydrology at this location, close to the partial ‘dams’ created for the Martock water intake (a DFO fish habitat offsetting project), and/or the extent of tidal influence. Some areas, including those where intentional seeding occurred on the floodplain (former intertidal flats) (Nikki-Marie Lloyd, CMM, personal communication, May 2022), remain sparse when compared to other areas, but were showing clear signs of growth.

Ecomorphodynamics

Based on the interpretation of satellite imagery from April to December 2021, with the re-introduction of partial tidal flow, intertidal flats were rapidly established with one narrow main river thalweg at low tide, and both appeared to remain stable throughout all time periods examined. Bathymetric analysis reported in van Proosdij et al. (2022) indicate that most sedimentation occurred within the first 450 m upstream section of the river, mostly in Lake Pisiquid (the head pond that formed behind the tide gates as a result of the installation of the causeway). However, quantifying changes in bathymetry and sediment volume are not possible within this report due to poor weather conditions and lack availability of survey equipment prior to winter. Sentinel-2 imagery using near infrared illustrates the expansion of vegetation between 5 May 2021 and 30 September 2022 and the marked reduction of bare ground.

Soils Characteristics

Fifteen of the 19 transect stations upstream of the causeway were dominated by cohesive sediments. The Munsell soil descriptions also indicate similarity between the cores. All share the same Hue of 7.5YR (yellow-red) and Value/Chroma ranging from brown (T461 4/4) to very dark brown (T2S5 2/3). Water content varied from 15% to 51% water content with highest values found in lower lying elevation zones. Organic matter content appears consistent between all the sites, with 13 out of the 16 sample locations ranging from 0% to 15%. There is no clear organic matter trend with station elevation. Bulk Density for the sites ranged from 0.456 to 1.393 g·cm^{-3}, with the lowest bulk density (0.456 g·cm^{-3}) recorded at T8S3 which is located furthest up the estuary, and the highest value (1.389 g·cm^{-3}) recorded at T3S6. Eight surface scrape samples were collected, mainly on the intertidal sand bar as well. All were within the fine sand category and the textural groups of the samples ranged from muddy sand to slightly gravelly sand. Soil characteristics were still showing influence from the previously established freshwater system, but were shifting towards a more estuarine characteristics with increasing contributions of fines.

Winter Conditions

A structured winter walk was conducted on 9 February 2023. Average temperatures recorded at the Kentville CDA CS weather station[1] for the 2022/23 winter season were below freezing for December (-2.2°C), January (-0.4°C), and until February 9th (-7.7°C). During the walk there was partial snow and ice coverage and ice slabs visible along the banks of the Avon River upstream of the tide gates.

Conclusions

This report provides documentation of the conditions existing upstream of the Windsor causeway during modified gate operations in the summer of 2022. They present a significant change in the ecological condition of the river following the implementation of the ministerial order requiring fish passage to the area above the causeway. With the head pond (Lake Pisiquid) drawn down and the river allowed to flow in a "more natural" way—in the sense that there is now some bidirectional flow and salt water has been re-introduced to a system that had been anthropogenically made freshwater— the hydrology is still primarily influenced by human activities. Operations of the gate in the current manner (prior to the 1 June 2023 closure order of the Avon River tide gates by EMO Minister John Lohr) has allowed for the development of dynamic wetland habitat upstream of the causeway, that range from salt through brackish to freshwater conditions. However, it should be noted that changes in operations will (and did) present another disruption in the ecosystem to once again shift these communities. Increased tidal inundation may result in increased dominance of halophytes in some areas and creation of new mudflat, while decreased tidal flooding could result in the reverse. Further, prolonged freshwater flooding if gates are closed is likely to lead to a rapid dieback of the vegetation communities that have established with implications to future soil formation in the river floodplain and future habitat conditions, productivity and biodiversity. As noted above, this situation has occurred and will not be resolved until both federal and provincial regulatory decisions are made concerning future operating conditions of the Avon River aboiteau system – current and planned future versions.

[1] https://climate.weather.gc.ca/historical_data/search_historic_data_e.html

1.0 INTRODUCTION

The Avon River and connected estuary is a very dynamic system and has a long history of morphodynamic and ecological change in response to natural and anthropogenic driving forces such as causeway construction, dredging, dyking, and sewage outflow modifications (van Proosdij and Baker, 2007; van Proosdij and Bowron, 2017). It is well known that the construction of causeways across tidal estuaries and rivers cause significant, often negative, impacts to the physical and biological conditions of the system (van Proosdij et al., 2009; Gerwing et al., 2017; Gerwing et al., 2020). While salt marshes and mudflat complexes often experience the most dramatic and observable effects caused by the change in the movement of water and sediment, upstream the Avon River Causeway has also been highly modified as a result of historical agricultural dyking, changing land use practices, hydroelectric dams, and the original causeway construction (i.e., converted to a freshwater head pond and river). After the construction of the Avon River causeway and tide gate between 1968 and 1970, the hydrodynamics and sediment transport processes were significantly altered, resulting in the rapid accumulation of fine sediments in the 1970s and '80s downstream of the causeway and creating the Windsor Marsh (additional details are provided in Graham et al., 2018 and van Proosdij et al., 2020). Since that time there has been significant changes in gate operations in order to allow fish passage (and more recently, reversion to a freshwater headpond).

Between 2016 and March 2021 the frequency of gate openings and tidal waters flowing upstream for short durations increased due to ongoing gate manipulations (Graeme Matheson, NSDA, personal communication, 28 February 2022). On 19 March 2021, a Ministerial order was issued by DFO Minister Bernadette Jordan dictating that the gates must be fully open during outgoing tides and open for a minimum of 10 mins on the incoming tides to allow salt water and fish passage upstream, that in turn impacted the ecomorphodynamics of the system. Detailed analysis of gate openings, sediment transport, and freshwater discharge are outside of the scope of the current study. While the historical downstream impacts of the construction of the causeway and the associated ecomorphodynamic adjustments in salt marsh habitat, tidal flats, and river channel are well documented (van Proosdij et al., 2006; van Proosdij and Baker, 2007; van Proosdij et al., 2009; van Proosdij and Bowron, 2017; Graham et al., 2018; van Proosdij et al., 2020.), there is little data available on the upstream impacts. Therefore, up to this point minimal analyses have been conducted upstream of the causeway structure. A previous report titled *Examination of the Morphodynamics of the Upstream Portion of the Avon River*, completed in March of 2022, provides some further background to the upstream conditions.

This report seeks to document the conditions upstream of the Avon River Causeway following the second year of Phase 1 construction as part of the Highway 101 Twinning Project and the application of the DFO Ministerial order. It is complementary to the report *Avon River Aboiteau and Causeway upgrades: 2022 Season Post-Construction Monitoring of the Windsor Marsh and Extended Baseline for Elderkin Marsh* (Kickbush et al., 2023).

1.1 Site Description

The study area extends approximately 7.2 km upstream from the existing causeway on the Avon River to Sangster's Bridge (Figure 1). Since the causeway was completed in 1970, freshwater discharge on the Avon River has been controlled by hydroelectric and storage dams in its upper reaches and by tide gates located within the Highway 101 (Avon River) causeway. The Avon Tide Gate was run on demand from its inception until 1981. This involved manually opening the gates fully on the outgoing tide when the lake level (area above causeway) and river (area below causeway) were equal. Since 1981, the gates have operated as an automatic system (with manual override) and are designed to maintain Lake Pisiquid (the head pond that formed behind the tide gates as a result of the installation of the causeway), at a set level. The lake was maintained at an operational elevation of 9 ft CGVD28, with levels fluctuating slightly seasonally and in response to specific needs (Graeme Matheson, NSDA, personal communication, September 2023). For example, Lake levels would be reduced typically in March to allow for maintenance of gate infrastructure (van Proosdij and Baker, 2007). Gates would also be opened periodically for short periods to accommodate spring movement of Gaspereau otherwise known as alewife (NSTIR, 2017). Sediment-laden tidal waters would move upstream during these periods as well. As previously mentioned, the frequency of gate openings and tidal water flowing upstream for short durations increased between 2016 and March 2021, with another change due to a DFO Ministerial order issued on 19 March 2021 dictating that the gates must be fully open during outgoing tides and open for a minimum of 10 min on the incoming tides to allow salt water and fish passage upstream.

2.0 RESEARCH METHODOLOGY

To document conditions upstream of the causeway, data was collected for a number of indicators that characterize the geomorphology, habitat, sediments and hydrological conditions of the study area. Collectively, these indicators provide a snapshot of the conditions resulting from several years of modified gate operations. The research methodology builds upon previous experience, and past downstream research and monitoring activities conducted by CBWES and SMU between 2002 and 2007, and 2017 to present (van Proosdij, 2005; van Proosdij et al., 2006b; van Proosdij and Baker, 2007; van Proosdij and Bowron, 2017; Graham et al, 2018; van Proosdij et al 2020; Kickbush et al, 2023). In addition, the indicators and data collection methods employed have been developed by the research team in environmental monitoring programs at tidal wetlands throughout the province, based in best practices regionally and internationally (Neckles et al., 2002; Bowron et al., 2012; NSTIR, 2017). The metrics and sampling methodologies are summarized in Table 1, with sampling locations shown in Figure 2. The following chapters will address each of the indicators listed in Table 1 based on the objective they are trying to achieve (e.g., Characterizing hydrology).

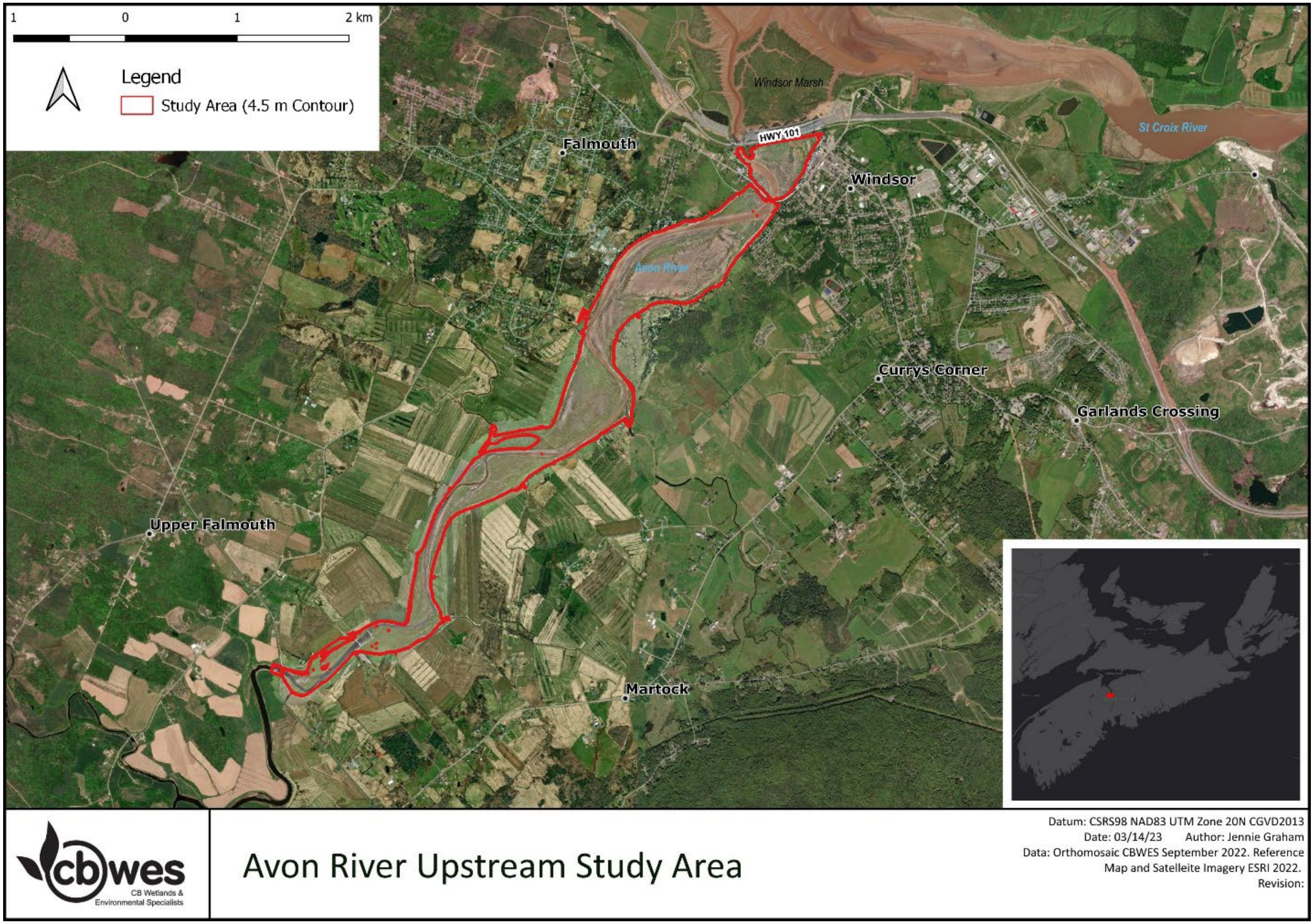

Figure 1: The study area, extending 7.2 km upstream from the existing causeway on the Avon River to Sangster's bridge.

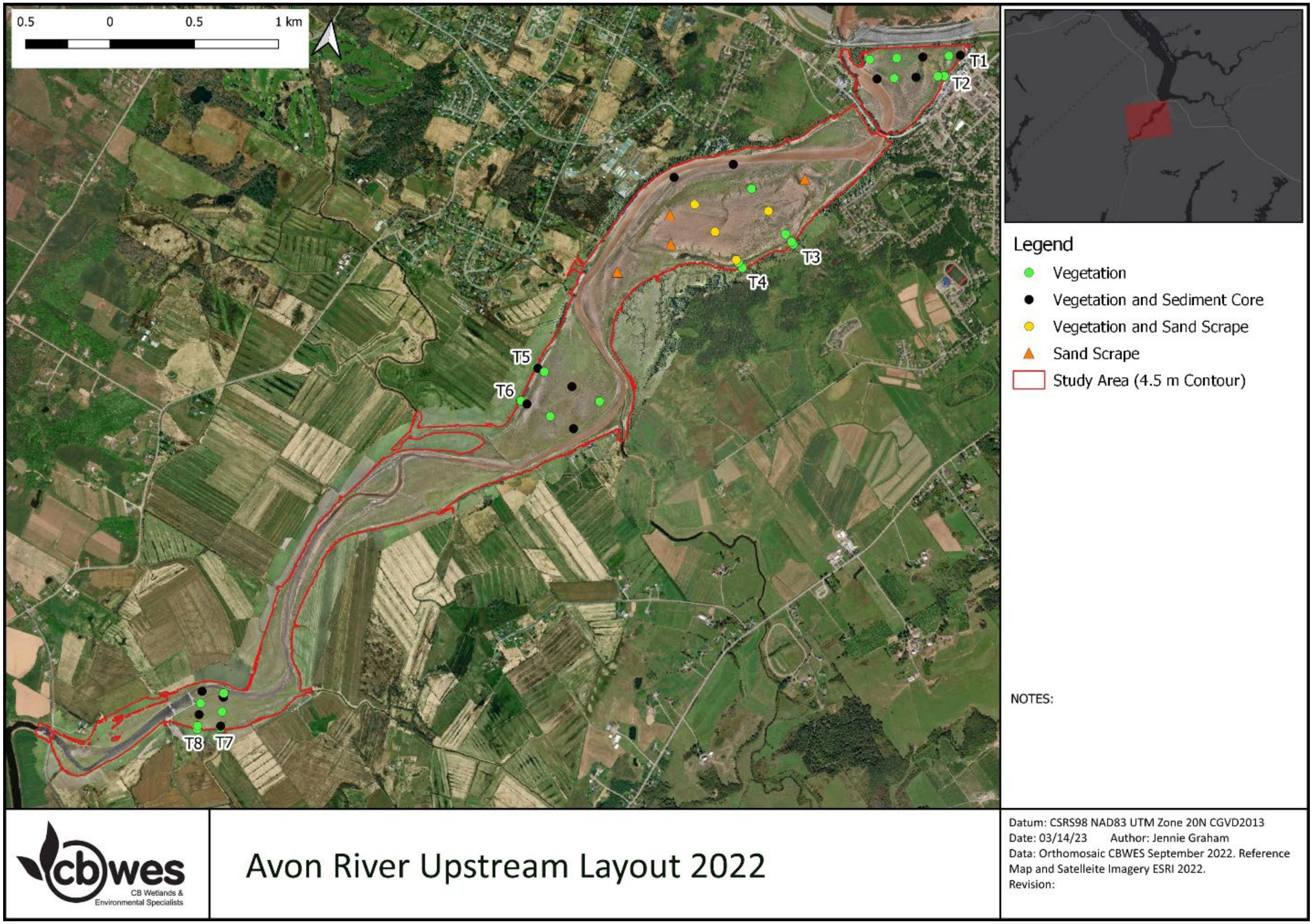

Figure 2: The study area, and I transects and sampling stations of the Avon River Upstream Layout, 2022.

Table 1: The Avon River Upstream monitoring program (✓ – completed sampling; Y – scheduled future sampling).

Objective	Indicator/Parameter	Sampling Method	Monitoring Year	
			2022	2023
Characterize Geomorphology	Marsh surface elevation	Digital Elevation Model (DEM/DSM); G8 GNSS RTK Sample Station Survey; Geo-referenced low-altitude aerial photography; Transect based elevation profiling;	✓	
	Bathymetry	Ship-based bathymetric survey		Y
Characterize Hydrology	Water level	Water level data from the Windsor tide gate station; Sample Station Elevation;	✓	
	Hydroperiod			
	Tidal flow patterns			
Characterize Habitat and Vegetation	Vegetation Composition	Transect based, Point Intercept Method (1 m^2 plots)	✓	
	Vegetation Abundance			
	Habitat map	DGPS/GIS; Geo-referenced low-altitude aerial photography	✓	
Characterize Sediments	Bulk density	Sediment cores; Sand grab; Multisizer 3 Coulter Counter;	✓	
	Organic matter content			
	Sediment type			
	Water content			
Characterize Ecomorphodynamics	Descriptive analysis	Sentinel Satellite Imagery; Geo-referenced low-altitude aerial photography	✓	
Evaluation of Growing Season Habitat	Visual Assessment of habitat condition, geomorphic change, wildlife usage, etc.	Structured summer walks & photo-documentation	✓	Y
Winter Conditions	Visual assessment of ice/snow, habitat conditions	Structured winter walk; photo-documentation	✓	Y

3.0 GEOMORPHOLOGY

Geomorphology is the study of landforms and the processes that shape them, and in this study, it is primarily characterized using geospatial data. Geospatial data include elevation survey data, Digital Elevation Models and Digital Surface Models (DEM, DSM), bathymetric survey data, and aerial photography. Additionally, geospatial data are used in other analysis—including hydrology, ecomorphodynamics, and habitat mapping.

3.1 Methods

RPAS Survey and Digital Surface Model (DSM)

Georeferenced low-altitude aerial photography was collected for Avon River Upstream (AVUS) on 10 May 2022 with the CBWES Inc.-Saint Mary's University (SMU) DJI Phantom 4 RTK[2] Remotely Piloted Aircraft System (RPAS) with an RGB camera, and on 7–8 September 2022 using the CBWES-SMU WingtraOne PPK[3] fixed-wing RPAS, with a Sony RX1R II 42 MP camera. Both data sets were collected during low tide, with the aboiteau gate open. The 10 May 2022 survey was flown only over a portion of the site (sand bar, Transects 3–4) at an altitude of 100 m above ground level (AGL), with a resulting pixel resolution of the output products of 0.030 m (Figure 3). The 7–8 September 2022 flight was flown at an altitude of 120 m AGL (WingtraOne PPK), with a resulting pixel resolution of the output products of 0.030 m. For both surveys, imagery was collected with a front overlap of 80% and a side overlap of 65%. Oblique imagery was obtained with the DJI Phantom 4 RTK RPAS on 12 September 2023 for supplementary qualitative analysis (Figure 4).

Prior to conducting the RPAS flights, Ground Control Point (GCP) networks were designed to ensure optimal georeferencing results in the Structure from Motion (SfM) workflow using the most up to date recommendations found in the scientific literature (James and Robson, 2014; Tonkin and Midgely, 2016; Raczynski, 2017). Additionally, both the DJI Phantom 4 RTK and WingtraOne PPK aircrafts come equipped with a GNSS antenna (Real-Time Kinematic and Post-Processing Kinematic, respectively), allowing for survey-grade positioning of collected imagery. This improved image positioning allows for more accurate georeferencing of SfM data products when used in combination with a well distributed GCP network. GCPs were deployed and surveyed using a Leica Geosystems GS14 dual-frequency GNSS receiver, which receives RTK corrections via the Leica SmartNet Correction Service over the TELUS cellular telephone network. Georeferenced orthomosaics and DSMs were generated using Agisoft Metashape software for each survey, and the orthomosaics were used as base imagery for all mapping tasks (e.g., habitat mapping, DEM analysis; geomorphic and anthropogenic feature identification). The highest accuracy settings were used for all steps of processing.

[2] https://www.dji.com/ca/phantom-4-rtk?site=brandsite&from=nav
[3] https://wingtra.com/mapping-drone-wingtraone/

The surfaces generated using RPAS imagery and SfM algorithms (Westoby et al., 2012) are DSMs, not bare earth elevation models (DEMs) because photogrammetrically-derived elevation models capture visible features only. Therefore, vegetation cover can obscure ground features, and ground surface elevations are only able to be measured when the ground is visible (areas of bare ground). DSMs can be useful in modeling elevations for inaccessible areas or those not easily surveyed (e.g., unconsolidated sediments) and provide additional information such as vegetation height and texture.

DSM accuracy can be reported using multiple metrics, including mean error, standard deviation (SD) of error, Mean Absolute Error (MAE), and Root Mean Squared Error (RMSE), which is the most commonly used metric in the literature. To estimate vertical DSM accuracy for the collected datasets, elevations of bare ground surfaces were measured with the GNSS receiver throughout the site subsequent to the aerial surveys. The Extract Multi Values to Points tool in ArcMap was used to append DSM elevations to the GNSS point data. DSM elevation values were then subtracted from the orthometric height values of the GNSS points to calculate vertical offsets, and the previously mentioned metrics were calculated to estimate DSM accuracies. RSME of the vertical component (RMSEz) is determined using the following equation (Hugenholtz et al., 2013):

$$RMSE_Z = \sqrt{\frac{1}{n}\sum_{i=1}^{n}(Z_{RTKi} - Z_{DSMi})^2}$$

Vertical errors of the AVUS DSMs were as follows:

DSM	N	Mean	SD	MAE	Min/Max	RSMEz
2022/05/10	65	-0.024	0.025	0.029	-0.072/0.034	0.034
2022/09/7-8	94	-0.041	0.039	0.043	-0.10/0.014	0.050

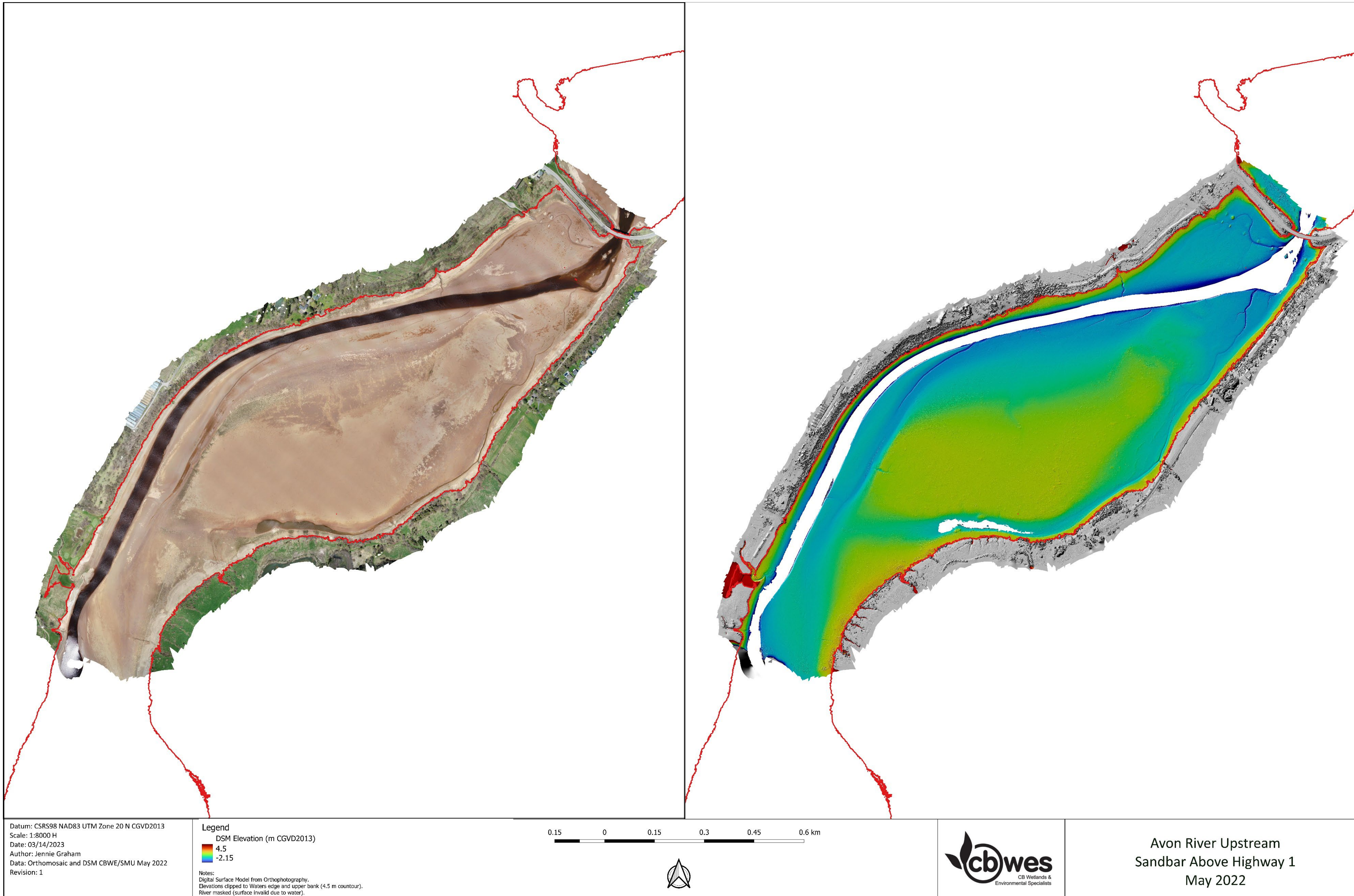

Figure 3: 2022 orthomosaic (left map) and DSM (right map) of the large sand bar on the Avon River upstream of the Trunk 1 bridge and causeway, May 2022.

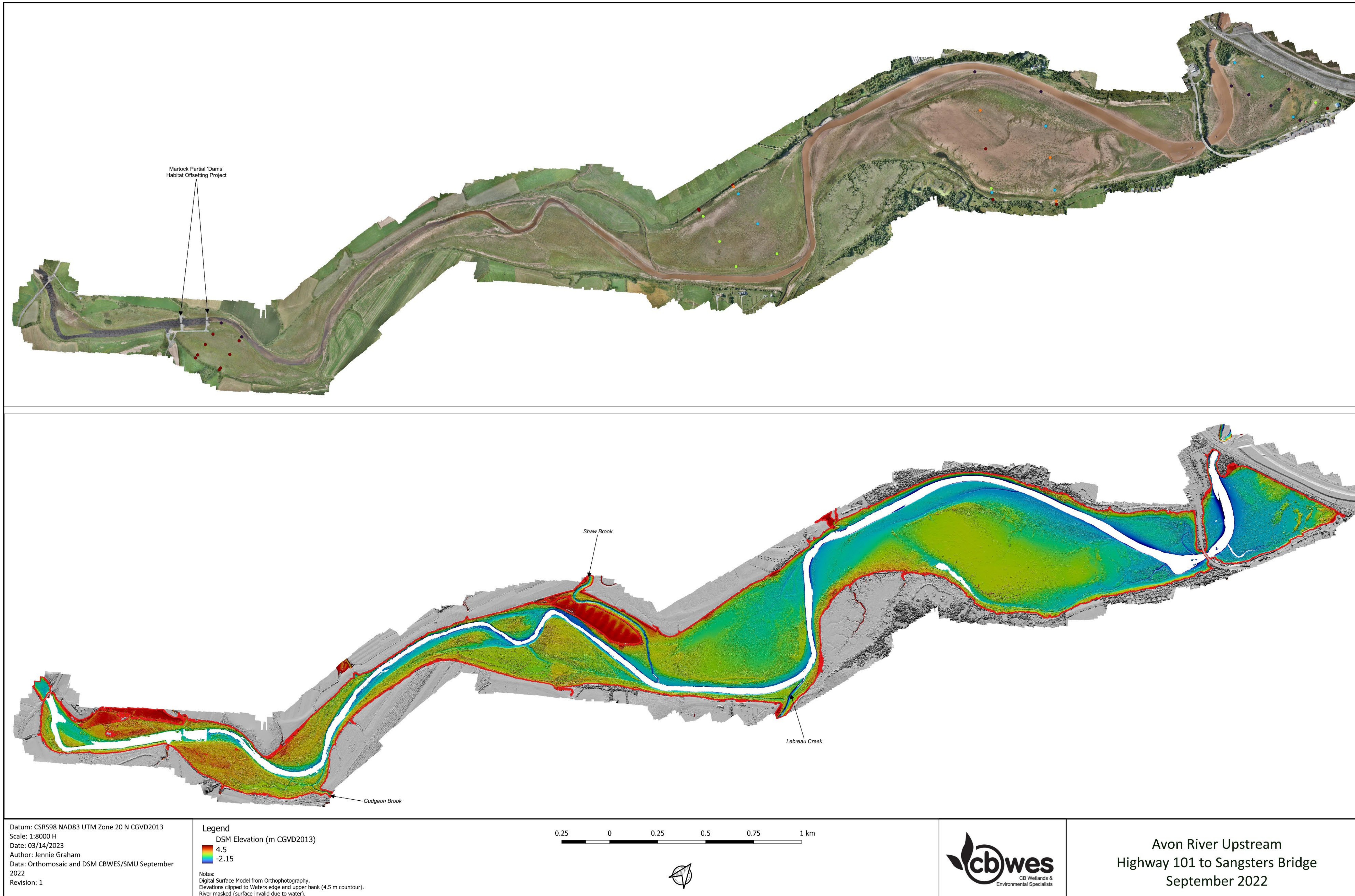

Figure 4: 2022 orthomosaic (upper map) and DSM (lower map) of the Avon River upstream of the Highway 101 Causeway to Sangster's Bridge, September 2022.

Elevation Survey

A series of eight transects, that transected the Avon River periodically, were used as the basis for the detailed elevation and vegetation surveys (Figure 1). Elevation data was collected along each transect, and at each station using a Leica Geosystems GS14 dual-frequency GNSS receiver described above. The 2022 Season data were collected on 12 August 2022 and 1 September 2022. The analysis started on the area immediately upstream and adjacent to the causeway and then proceeded at intervals up the Avon River to capture areas of significance. GNSS survey data were combined with a 2019 DSM with partial site coverage, and the September 2022 DSM to generate elevation profiles (Figure 5).

3.2 Results and Discussion

The aerial photography, DSM and elevation transects show that the study area is characterized by a narrow river channel and a wide, relatively flat floodplain (former riverbed/tidal mud flat). The floodplain, whose upland boundaries are the historic banks of the Avon River, widens as one moves downstream from Sangster's Bridge to the Avon River Causeway. The morphology is typical for tidal rivers in the Bay of Fundy.

Comparing the 2022 DSM to the 2022 GNSS points (ground surface elevations) shows that the floodplain was heavily vegetated in September 2022 (Figure 5). When surveyed points were compared to the corresponding DSM elevation, there was a mean difference of 32 cm ± 31 cm, with a median value of 19 cm—indicating that 50% of the surveyed points were collected in areas that were either bare ground, low growing vegetation, or sparsely vegetated areas. The maximum difference was 1.36 m, which occurred in a dense stand of *Schoenoplectus tabernaemontani* on Transect 2. While the tallest vegetation was found on Transect 2, mean vegetation height is greatest along transects T7 and T8, furthest away from tidal influence and at higher elevations than transects lower in the estuary. This is also evident in the transect profiles. The separation between the ground and DSM surface on T1 is greater in some spaces but patchy, reflecting plant communities of variable height interspersed with bare ground. Along T7 and T8 the separation is smaller (vegetation is shorter) but very consistent. The lowest density of vegetation coverage occurs around Transects 3 and 4, which coincides with a large sand bar, referred to as the "Windsor Sandbar". The bar, which is markedly different in sediment composition and at a higher elevation given its location in the river, was slow to green up and remained less densely vegetated than other areas of the site at the time of the flight (Figure 6). Further discussion of vegetation dynamics is provided in *5.0 Vegetation and Habitat.* Station elevations (Figure 5) range between -1.156 m and 4.198 m CGVD2013, with a mean elevation of 0.718 ± 1.014 m.

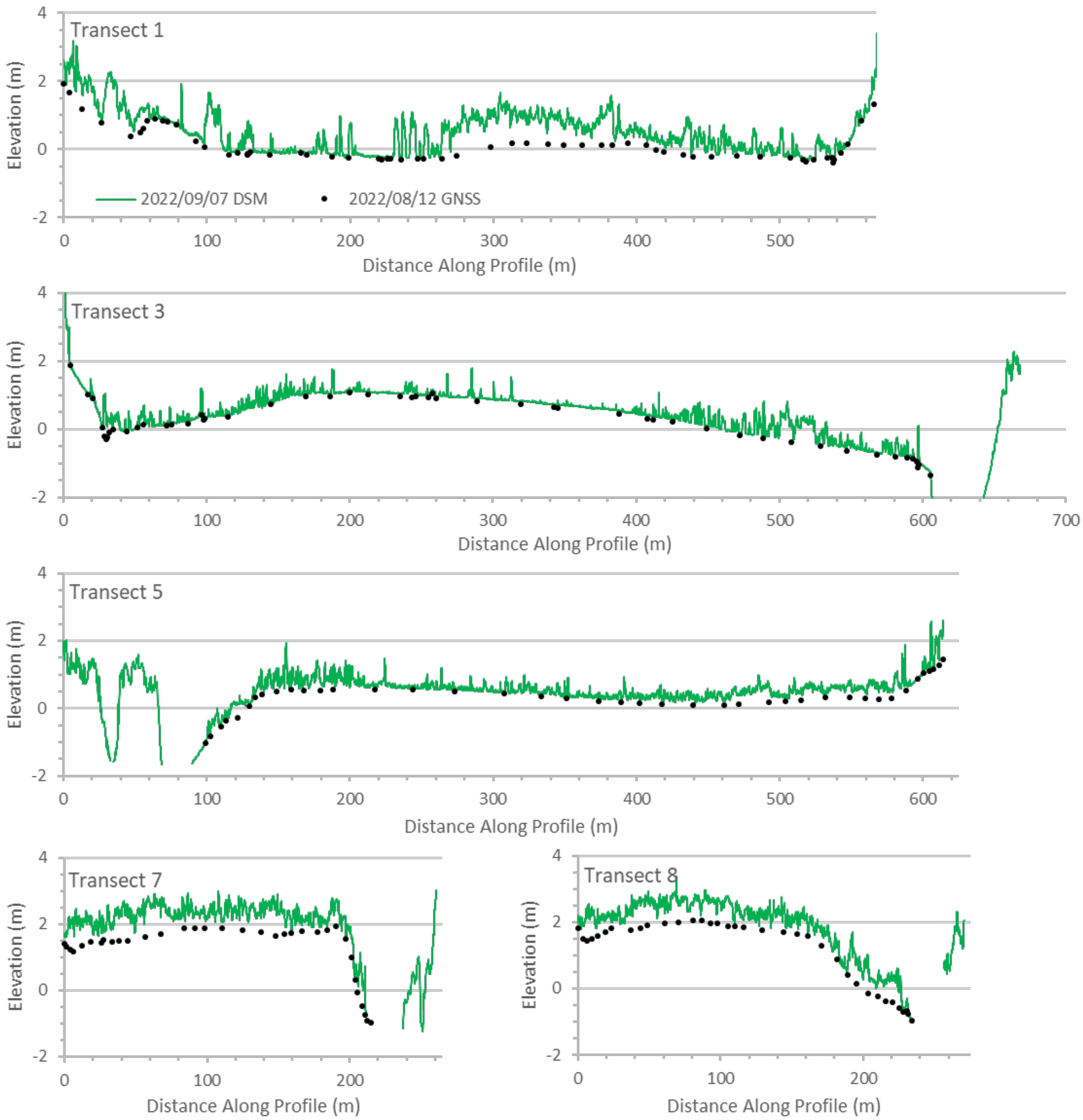

Figure 5: Surveyed elevations of Transects 1, 3, 5, 7, and 8 at the Avon River Upstream study site with DSM surface overlaid. All transects extend from East to West, and elevations are reported in CGVD2013. Vertical exaggeration = 35.6. See Figure 1 for transect locations. Black dots = GNSS ground survey; Green Line = DSM surface, including height of the vegetation.

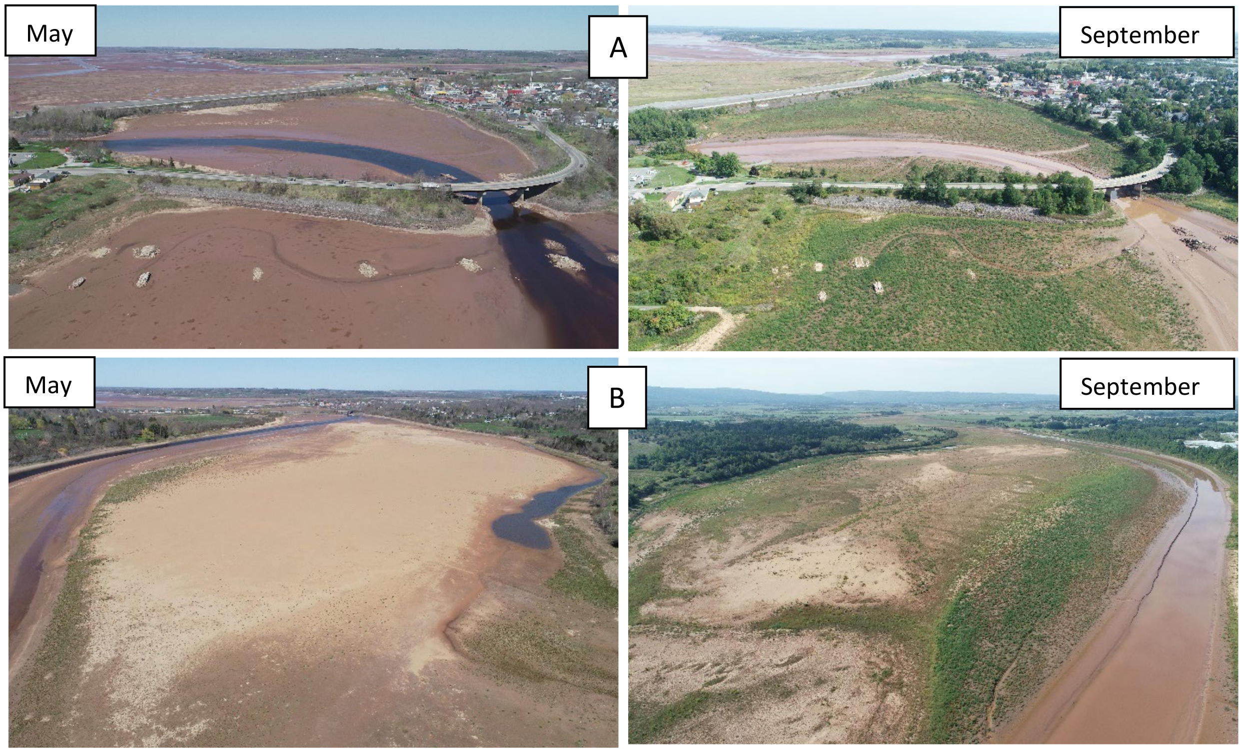

Figure 6: A) Aerial view of river immediate upstream of Highway 101 (T1 & T2) and B) Large sandbar (the "Windsor Sandbar") (T2 & T3) in May (left) and September (right), 2022. Note September image facing upstream (Southwest). All others facing downstream.

Table 2: Statistics for AVUS station elevation survey, 12 August 2022 and 1 Sept 2022. Elevations are reported in CGVD2013.

	Station Elevation (m)
Min	-1.156
Max	4.198
Mean	0.718
SD	1.014

4.0 HYDROLOGY

Hydrology is the study of water on and beneath the earth's surface, including its movement in relation to living (biotic) and material (abiotic) components of the environment (Bales, 2015). Hydrology is a fundamental control on the structure and function of wetlands, and the introduction of tidal flooding (salt water) is a critical component of tidal wetlands (Mitsch and Gosselink, 1986; Neckles and Dionne, 2000). Manipulations of the gate have had a dramatic effect on the ecosystem upstream of the highway, transitioning the habitat from an artificial lake (head pond) to a river, wetland and mudflat/sandflat complex. This section of the analysis seeks to characterize the new hydrology of the system.

4.1 Methods

Water levels recorded upstream and downstream of the Avon River Causeway were obtained from NSDA for the period of 1 January 2021 to 31 December 2022. The downstream water level logger (pressure transducer) was located within the aboiteau culvert and immediately downstream from Gate 1. The upstream logger (sonar system) was mounted on the underside of the Trunk 1 Bridge over Lake Pisiquid, ~600 m from the gate. Both loggers were set to record at 1-minute intervals, and were unable to record water levels below 1.95 m CGVD2013. Erroneous data that was a result of ice on the logger or power outages, and therefore incorrect, were manually removed from the dataset (e.g., 1 December 2022). Tidal signal graphs were generated, and the data used to calculate min/mean/max tide levels and mean water levels.

Changes in water level have a direct impact on the habitat within the site. Hydroperiod and inundation frequency (frequency and duration of flooding) play a crucial role in processes such as sedimentation, soil development, vegetation zonation, and carbon sequestration. The hydroperiod is determined by the water level relative to ground elevation at surveyed vegetation stations. Three statistics were calculated: Inundation Ratio (IR: time during the recording period the station was flooded), Inundation Frequency (IF: percent of high tides which inundate station regardless of duration of flooding), and Mean Inundation Time (MIT: average duration of inundation when it occurs, calculated by dividing time flooded by number of events reaching station). These values are calculated based on the water levels recorded by the logger located at the Trunk 1 bridge and assume that a station will flood if it lies below the water level, regardless of connectivity to the river and distance to the water level recorder. As a result, hydroperiod statistics should be interpreted with caution—they provide a general characterization for each station but become less reliable with distance from the logger.

It should also be noted that the Avon River estuarine hydrological system is complex, with not only the enormous natural variations in tides which are inherent in the Bay of Fundy—particularly the Minas Basin—but also have the added complexity of high anthropogenic manipulation. As previously mentioned in the *Introduction* and *Site Description*, the causeway and tide gates across the Avon River has resulted in controlled water levels upstream based on the objectives of the tide gate operators, rather than by the natural tidal-freshwater flux of an open estuarine river system. For many years, upstream water levels were determined by linked objectives to maintain the desired freshwater levels to sustain Lake Pisiquid (the headpond), and response to fluctuations in the operations of the NS Power hydroelectric dam system further upstream, and therefore had minimal upstream saltwater flow. More recently, the objectives of the operation of the tide gate have shifted and set to allow saltwater flow upstream and improved fish passage for at least 10 mins during incoming tides.

4.2 Results and Discussion

Water levels for the period of 1 January to 31 December 2022, are shown in Figure 7 with precipitation from the Kentville climate station[4]. Daily water fluctuations upstream of the causeway were most heavily influenced by the incoming tide, increasing rapidly until the tide gate was shut (Figure 8). The water levels then increase slowly as freshwater is not discharged during the high tide period. When the downstream tide levels fall to a level equal to the upstream water level, the tide gates are opened once again, and water levels drop both upstream and downstream. The average water level during the high tide period upstream of the aboiteau was -0.57 m CGVD2013 ± 0.54 m, while downstream it was 5.8 m CGVD2013 ± 0.79 m.

While daily upstream water levels were most heavily impacted by the tide gate operation, the highest water level of 3.1 m CGVD2013 occurred on 18 February 2022 (see Figure 8), and was a result of NS Power spilling the upstream dams coinciding with a high precipitation event (27.8 mm; Graeme Matheson, NSDA, personal communication, March 2023). This anthropogenic event resulted in water levels that were approximately 5 times the average water level upstream at high tide. The highest tide elevation downstream of the causeway, which was 7.5 m on January 2nd, did not occur at the same time. Because the loggers did not capture water levels below an elevation of -1.95 m CGVD2013, low tide levels were not recorded downstream of the aboiteau (i.e., the logger was not submerged during low tide; see Figure 7 and Figure 8). While at times, the upstream loggers did capture water levels while the tide was out and the gates were open (i.e., base flow when more fresh water was in the system), base flow was not captured during drier times of the year. Increased water levels during low tide periods could have occurred because of precipitation or because NS Power had spilled the upstream dam.

Hydroperiod statistics (IR, IF, and MIT) were calculated for surveyed stations to better understand potential inundation patterns (Figure 9, Table 3). IR and IF are high for low elevation stations and generally decrease moving upstream and towards the upland edge as elevation increases. Transects T5 and T6 have the lowest mean IR and IF values, though they do not have the highest mean elevation—the highest mean elevation was found along T7 and T8. This is because the elevation range of stations sampled was smaller along T5 and T6 than T7 and T8. Transect 2 had the highest mean IF and IR, with the lowest mean elevation and elevation range sampled. It's also worth noting that while stations at lower elevations have long mean inundation times (e.g., T2S5 is flooded for a long period when the gate is closed during most high tides), some stations at higher elevations (above ~ 0.5 m) also have higher than expected inundation time because the stations were flooded for an extended period during extreme high water events such as that on February 18th and rarely or not at all during "normal" gate closures (e.g., T4S3 flooded only 5 times but for long periods).

[4] https://climate.weather.gc.ca/climate_data/daily_data_e.html?StationID=27141

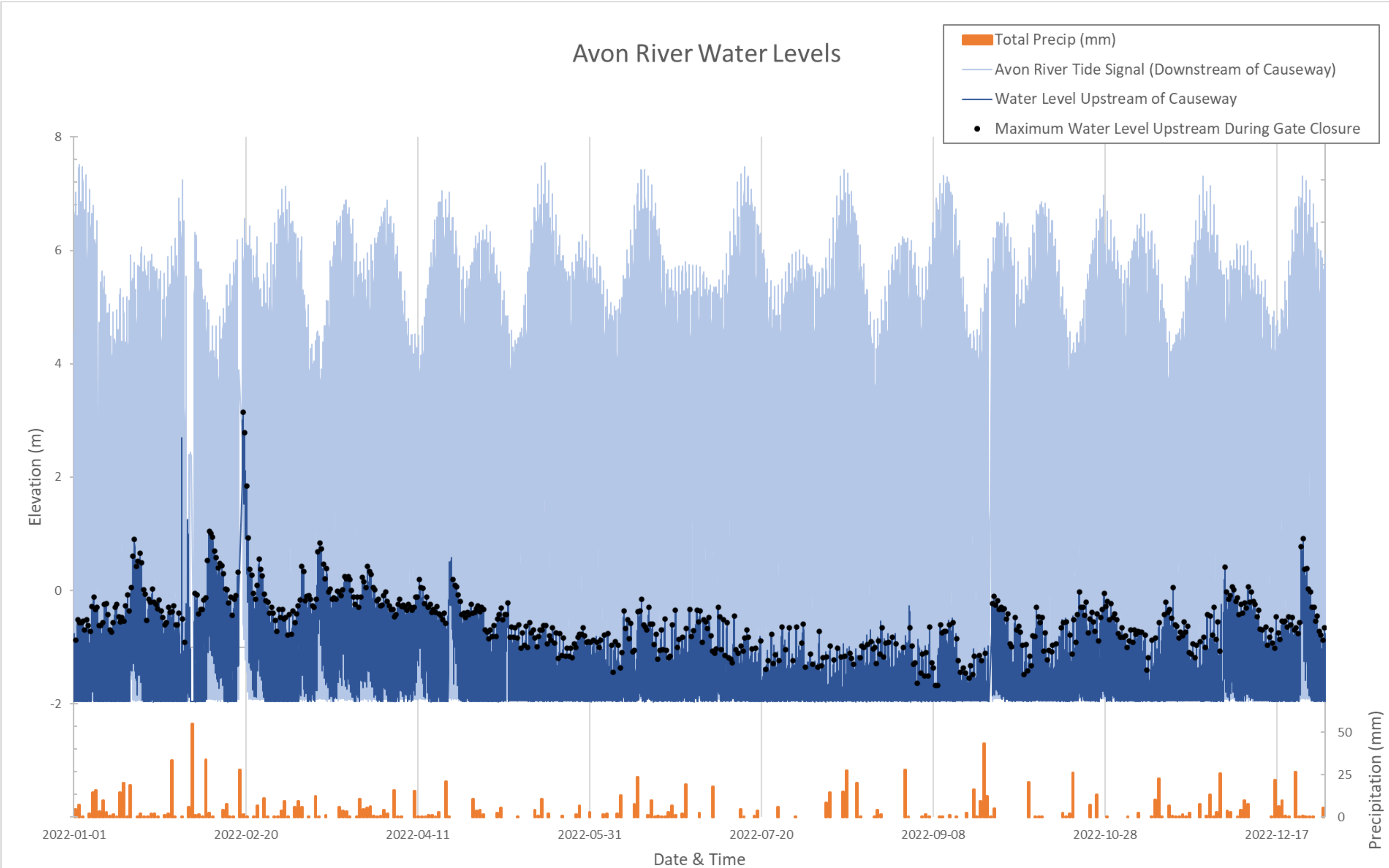

Figure 7: Tidal Signal for the High Tides of Avon River Upstream at the Highway 1 Bridge and Downstream of the Causeway in the Avon River within aboiteau 2021-2022; water level data courtesy of NSDA.

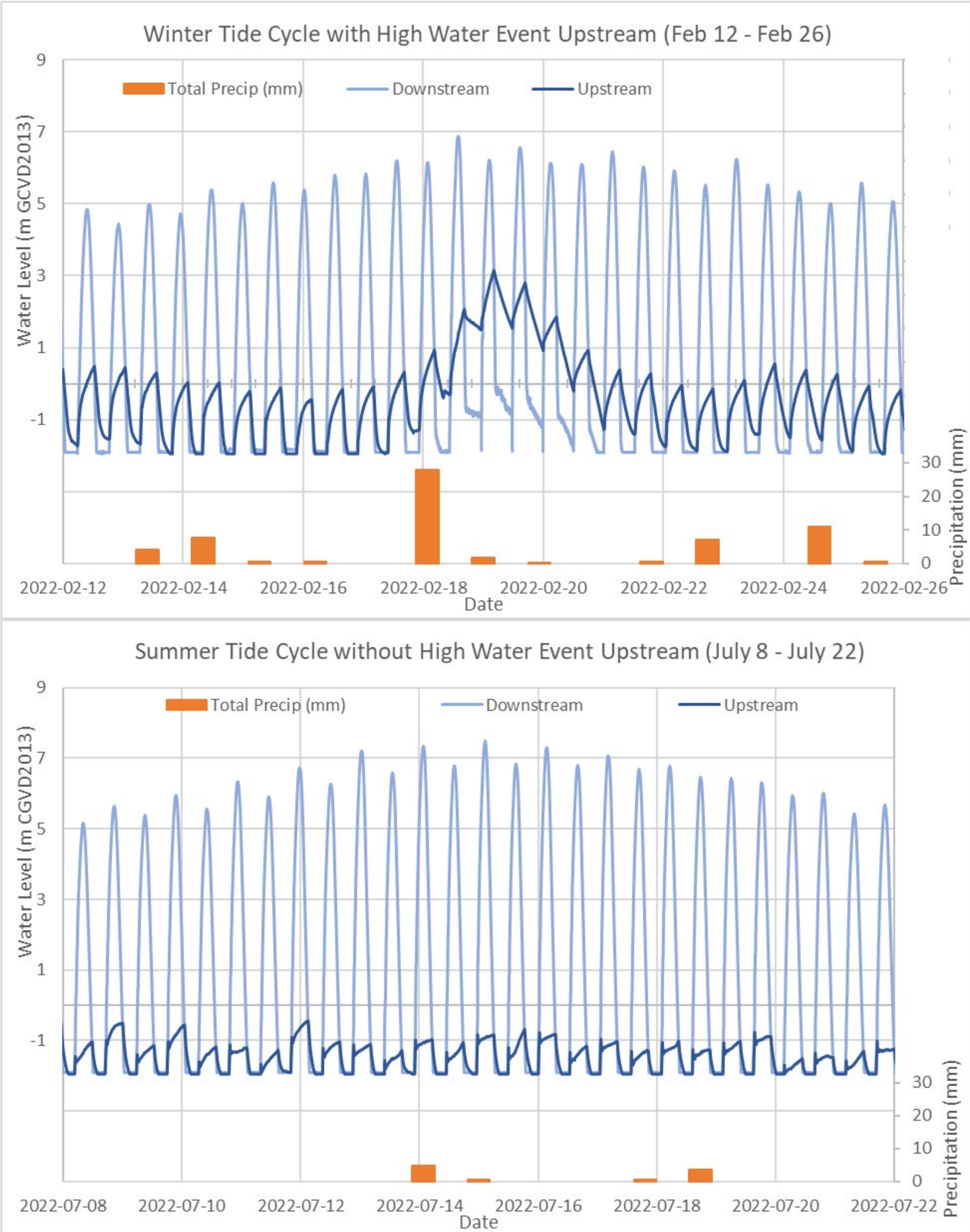

Figure 8: Winter and Summer tide cycle and effects of precipitation events

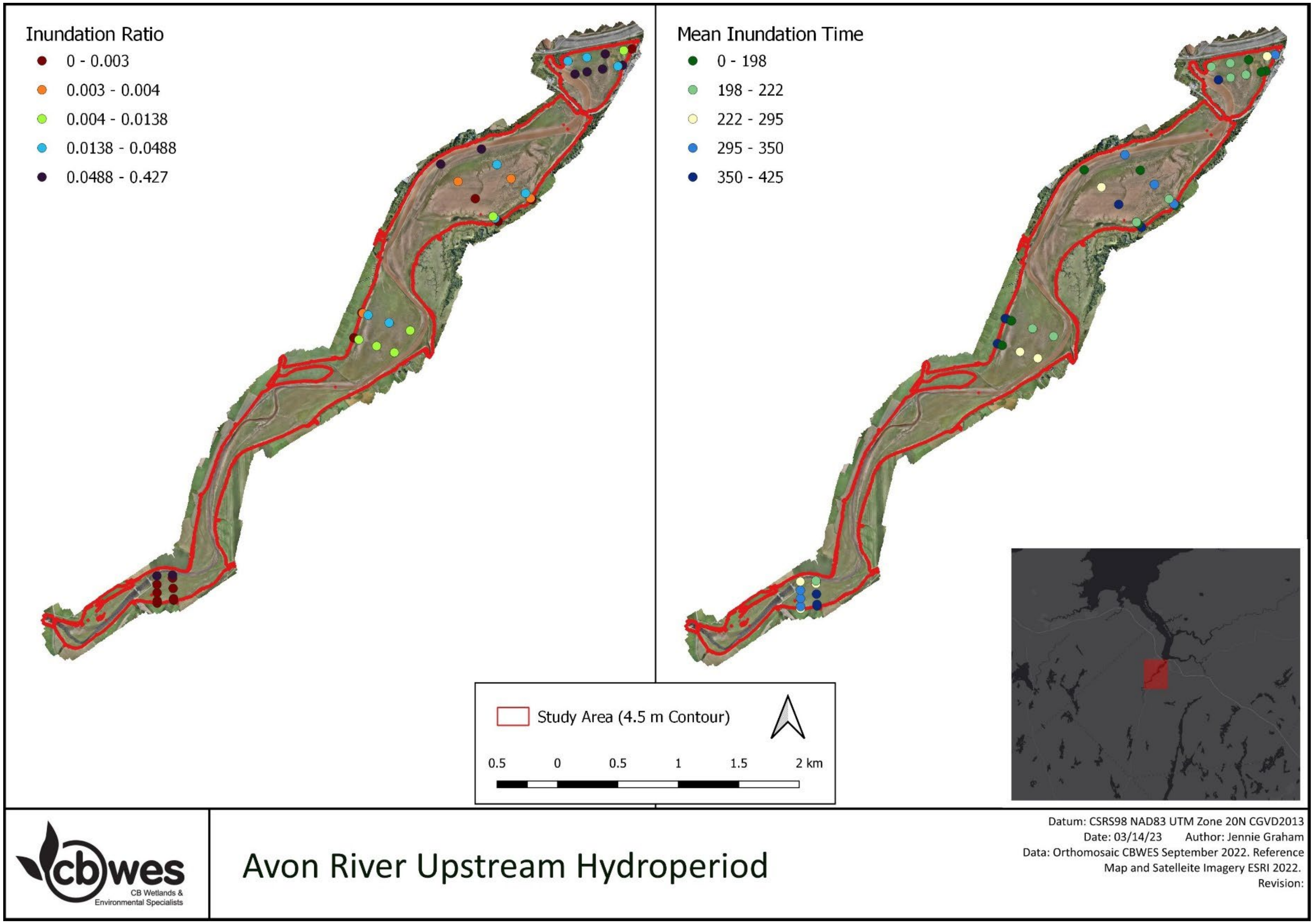

Figure 9: Hydroperiod for Avone River Upsteram of causeway: Inundation Ratio (Left) and Mean Inundation Time (minutes) (right).

Table 3: Hydroperiod Statistics by transect for 2022

Transect	Mean Elevation + Standard deviation (m CGVD2013)	Mean Inundation Ratio (IR)	Mean Inundation Frequency (IF %)	Average of Mean Inundation time (min)
T1	0.44 ± 0.81	0.027	10.0	234
T2	-0.49 ± 0.39	0.149	40.9	234
T3	0.94 ± 0.77	0.055	14.2	230
T4	0.61 ± 0.76	0.025	9.1	266
T5	0.72 ± 0.53	0.009	3.4	275
T6	0.96 ± 0.51	0.006	1.9	282
T7	1.2 ± 0.97	0.025	8.4	334
T8	1.33 ± 1.08	0.032	9.9	298
All stations	0.72 ± 0.63	0.041	12.188	268

5.0 VEGETATION AND HABITAT

The 1968-1970s construction of the Avon River tide gate and causeway facilitated the upstream shift from tidal to freshwater system including a freshwater headpond (Lake Pisiquid) directly upstream of the tidal gate while downstream there was rapid sedimentation and formation of a significant tidal flat (van Proosdij and Townsend, 2006; Daborn et al., 2003; van Proosdij and Baker, 2007). After the DFO Ministerial Order in March of 2021, that required the river to be returned to “a more natural river state” by changing tide gate operations as described in section *1.0 Introduction*, sand bars and flats were exposed along 7 km of the river upstream of the causeway. While incoming tidal flow has been allowed for at least 10 minutes at each tide, the Avon River remains significantly tidally restricted, resulting in the sand bars remaining exposed for long periods. Vegetation distribution and community composition is influenced by the frequency and duration of flooding. For the first year (2021) of the Ministerial Order, saltwater entry exceeded the 10-minute requirement and resulted in the establishment of some vegetation on the newly exposed sandbars and mudflats, and wetting of the flats (Lloyd, 2022). Further changes were made to the tide gate schedule in 2022 and the Province reduced the flow to near the minimum allowance (Lloyd, 2022). In 2022 new vegetation growth was slow, and vegetation remained sparse on the sandbars and mudflats—potentially in conjunction with reduced flooding from incoming tidal flow compared to 2021—that may have contributed to the mobilization of fine sandy dry loose sediments by the wind and became a dust issue for local residents.

In response to this dust issue, an appropriate solution to help prevent the mobilization of fine sediments from the sand bar was developed to seed the sandbar, giving the vegetation that would eventually naturally establish a “head start”. The seeding of the sandbar project (henceforth referred to as “the Seeding Project”) was led by the Confederacy of Mainland Mi’kmaq (CMM) and was in partnership with DFO, NSDA, CBWES, Kwilmu’kw Maw-Klusuaqn Negotiations Office (KMKNO) and commercial fisher, Darren Porter. On 13 May 2022, ~ 13 ha of the 43 ha “Windsor bar” (the largest of the exposed sandbars upstream of Highway 1) was seeded with a highway seed mix (Nikki-Marie Lloyd, CMM, personal communication, May 2022). Additional hand seeding and live transplants on the bar were conducted on 11 June 2022 as part of a community volunteer event hosted by CMM.[5]

For this report, point intercept vegetation surveys were used to understand species richness, diversity and distribution. Habitat mapping was carried out using low-altitude aerial photography to generate broad vegetation cover classes, with the point intercept data used to inform habitat interpretation. The area of the Seeding Project is captured by the methodology used in this report and is included in the results of this section. It should be noted that it was less than a full growing season between the implementation of the Seeding Project (May and June) and the low-altitude aerial photography and vegetation surveys (September). Additional photos were captured during the collection of sediment samples later in the fall. These observations are further discussed below in the habitat mapping results section.

5.1 Methods

Vegetation Surveys

Plant species richness, halophytic species, and abundance, and unvegetated area in 1 m^2 plots were assessed at the Avon Upstream site on 1–2 September 2022. Plant species abundances in plots were assessed as the number of pins contacted by leaves/stems/flowers out of a total of 25 pins in a 5 x 5 grid of 20 cm squares; total number of contacts per species was multiplied by four to yield a percent cover estimate (x/25 * 100). Halophytic species abundance was estimated as the total number of contact points by halophytic species per plot to a maximum of 25. The species encountered at these sites that were classified as halophytes are: *Atriplex* spp., *Carex paleacea, Juncus gerardii, Plantago maritima, Solidago sempervirens, Sporobolus alterniflorus, Sporobolus, Spergularia salina, Suaeda maritima*, and *Triglochin maritima*. None of these species were present in the "highway seed mix" and represent natural colonizers reaching the mudflat from nearby seedbanks (e.g. downstream salt marsh).

In order to determine the wetland indicator status of each plot, the Nova Scotia Environment and Climate Change indicator plant list was used to assign a score to each species as a quantification of its wetland indicator status, an ordinal scale with nine values (Table 4). The average of all species per plot was then calculated as the plot level wetland indicator status. Non-metric multidimensional scaling ordination was used to compare species composition and abundance between plots.

[5] For more information on the seeding project and the subsequent volunteer event, please contact CMM (https://cmmns.com/contact/)

Table 4: Wetland indicator status and equivalent quantitative score used to evaluate vegetation plots.

Status	Score	Status	Score
OBL (obligate wetland)	4	FAC (Facultative)	0
FACW+ (Facultative wetland +)	3	FACU+ (Facultative upland +)	-1
FACW (Facultative wetland)	2	FACU (Facultative upland)	-2
FACW- (Facultative wetland -)	1	FACU- (Facultative upland -)	-3

Habitat Mapping

Image segmentation and classification were carried out for the 7 September 2022 orthomosaic in QGIS using the Orfeo Toolbox (OTB) and, using vegetation survey data to aid in assigning classes to specific vegetation communities. The classification was constrained to areas below the 4.5 m contour, limiting the classification to the floodplain area. Due to the diversity of species and limited spatial extent of vegetation data collection, only 3 classes were generated: vegetated area; sparsely vegetated area; and a combined class of bare ground, built features, water, and the Seeding Project area. Expert interpretation was used than to identify and delineate built features, water, and the Seeding Project (which could not be differentiated from bare ground by the decision tree vector classifier used). Additional manual cleaning and improvement to the classification were carried out where needed. Mean wetland index, species count, and dominant species cover at point intercept pots were mapped with the classification to allow for additional qualitative interpretation of habitats within the Avon River area.

5.2 Results and Discussion

Vegetation Surveys

In 2022, AVUS contained a variety of vegetation that encompasses species from a variety of habitats: wet meadow, freshwater marsh, salt marsh and a handful of weedy (ruderal or first colonizer) species (Figure 10, Table 5). There were many plots, especially at lower elevations with high scores for wetland indicator status. The lowest scores were still in the facultative wetland category, indicating that plants with an affinity for wet sites are dominant here. Halophytes were abundant at the site, with an average of 23% coverage across all plots. Freshwater and salt-tolerant wetland species coexisted in the same plots (e.g., *Typha* and *Sporobolus alterniflorus*; Figure 10) indicating that typical salt marsh zonation has not occurred. The main dominant species were native (*Eleocharis palustris, Leerzia oryzoides, Phalaris arundinacea, Sporobolus michauxianus*).

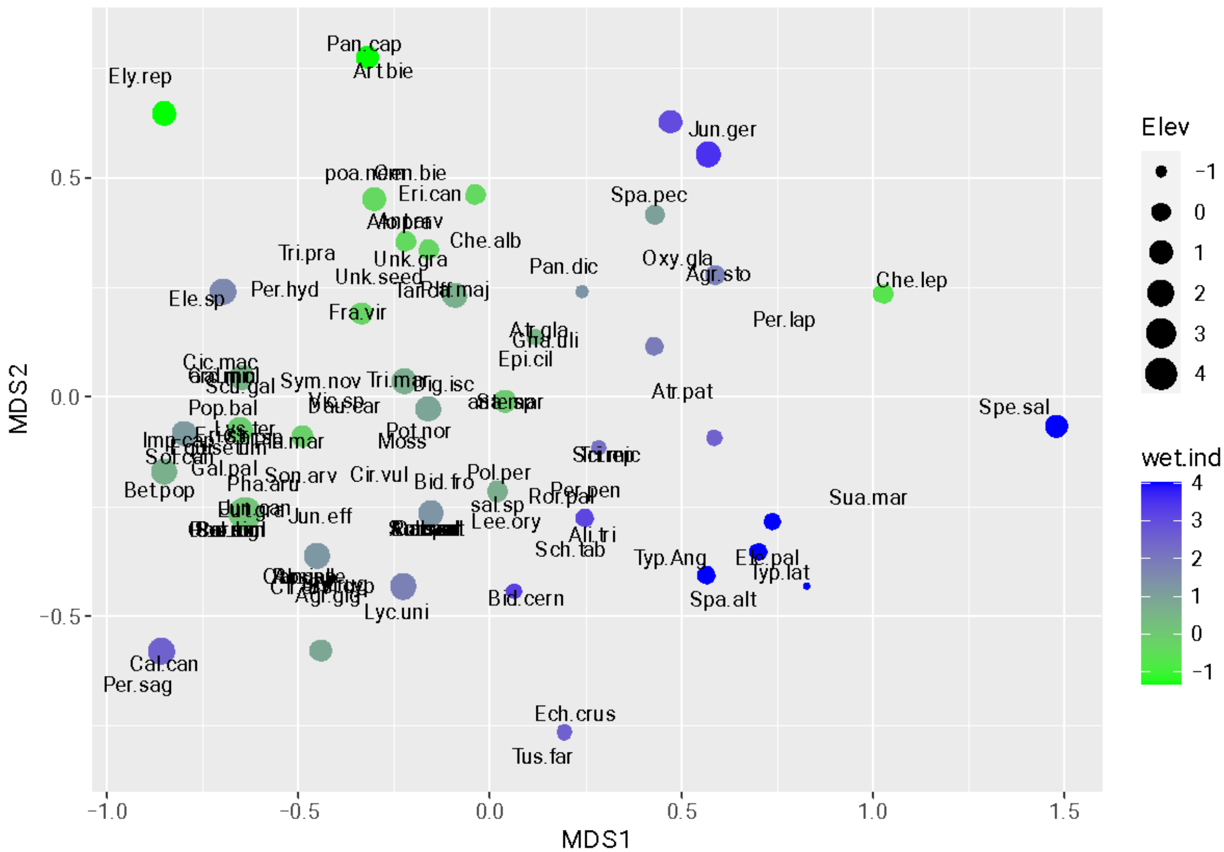

Figure 10: Non-metric multidimensional scaling ordination (stress = 0.15) using plant species cover values from vegetation plots at AVUS. Plots are represented by circles. Species scores are indicated by codes (Table 4). The relative size of the circle is proportional to plot elevation (larger circles = higher elevations). The colour indicates the average wetland indicator status of the species found in the plot with blue being the highest and green being the lowest.

Table 5: Plant species average plot coverage and frequency at AVUS in 2022.

Species	Code	% Cover	No. plots
Agrostis gigantea	Agr.gig	0.4	3
Agrostis stolonifera	Agr.sto	2.57	2
Alisma triviale	Ali.tri	0.02	1
Alnus incana	Aln.inc	0.19	1
Alopecurus pratensis	Alo.pra	0.29	1
Ambrosia artemisiifolia	Amb.art	0.1	1
Anaphalis margaritacea	ana.mar	0.02	1
Anthemis arvensis	Ant.arv	5.67	8
Arctium minus	arc.min	0.1	1
Artemisia biennis	Art.bie	0.6	3
Atriplex glabriuscula	Atr.gla	0.02	1
Atriplex patula	Atr.pat	4	6

Species	Code	% Cover	No. plots
Betula populifolia	Bet.pop	2.43	4
Bidens cernua	Bid.cern	0.12	2
Bidens frondose	Bid.fro	6.6	17
Calamagrostis canadensis	Cal.can	3.62	3
Carex lurida	Car.lur	0.57	1
Carex paleacea	Car.pal	0.38	1
Carex pallescens	Car.palle	0.38	1
Carex sp.	Car.sp	1.26	3
Carex vulpinoidea	Car.vul	0.57	1
Chenopodium album	Che.alb	6.5	9
Chenopodium leptophyllum	Che.lep	0.19	1
Cicuta maculate	Cic.mac	0.4	2
Cirsium arvense	Cir.arv	0.38	2
Cirsium vulgare	Cir.vul	0.48	2
Daucus carota	Dau.car	1.14	5
Digitaria ischaemum	Dig.isc	0.5	3
Echinochloa crus-galli	Ech.crus	0.88	3
Eleocharis palustris	Ele.pal	11.83	10
Eleocharis sp.	Ele.sp	2.19	2
Elymus repens	Ely.rep	0.38	1
Epilobium ciliatum	Epi.cil	0.05	2
Equisetum sp.	Equisetum	0.57	2
Erigeron canadensis	Eri.can	0.31	3
Erigeron strigosus	Eri.str	0.38	1
Euthamia graminifolia	Eut.gra	5.74	10
Fragaria virginiana	Fra.vir	0.12	2
Galium mollugo	Gal.mol	0.48	1
Galium palustre	Gal.pal	0.31	3
Gnaphalium uliginosum	Gna.uli	0.21	2
Impatiens capensis	Imp.cap	0.5	3
Juncus canadensis	Jun.can	4.1	2
Juncus effusus	Jun.eff	4.98	5
Juncus gerardii	Jun.ger	0.21	2
Leersia oryzoides	Lee.ory	12.19	11
Lycopus uniflorus	Lyc.uni	0.02	1
Lysimachia terrestris	Lys.ter	0.12	2
Moss	Moss	0.48	3

Species	Code	% Cover	No. plots
Oenothera biennis	Oen.bie	0.6	3
Onoclea sensibilis	Ono.sen	0.02	1
Oxybasis glauca	Oxy.gla	1.9	4
Panicum capillare	Pan.cap	1.55	4
Panicum dichotomiflorum ssp. *dichotomiflorum*	Pan.dic	3.86	10
Persicaria hydropiper	Per.hyd	4.38	8
Persicaria lapathifolia	Per.lap	1.74	6
Persicaria pensylvanica	Per.pen	0.57	3
Persicaria sagittate	Per.sag	0.1	1
Phalaris arundinacea	Pha.aru	11.62	12
Plantago major	Pla.maj	2.4	7
Plantago maritima	Pla.mar	0.1	1
Poa nemoralis	poa.nem	0.1	1
Persicaria maculosa	Pol.per	0.12	2
Populus balsamifera	Pop.bal	0.05	2
Potentilla norvegica	Pot.nor	0.24	3
Rorippa palustris	Ror.pal	0.4	3
Rosa multiflora	Ros.mul	0.76	1
Rosa sp.	Ros.sp	0.19	1
Rumex crispus	Rum.cri	0.1	1
Salix sp.	sal.sp	0.57	1
Schoenoplectus tabernaemontani	Sch.tab	5.33	9
Scirpus cyperinus	Sci.cyp	5.05	5
Scirpus microcarpus	Sci.mic	1.05	1
Scutellaria galericulata	Scu.gal	0.19	2
Solidago canadensis	Sol.can	1.62	5
Solanum nigrum	Sol.nig	0.19	1
Solidago rugosa	Sol.rug	1.14	4
Solidago sempervirens	Sol.sem	0.1	1
Sonchus arvensis	Son.arv	2.14	9
Sporobolus alterniflorus	Spa.alt	1.24	1
Sporobolus michauxianus	Spa.pec	13.14	13
Spergularia salina	Spe.sal	3.33	4
Stellaria sp.	Ste.sp	0.02	1
Suaeda maritima spp maritima	Sua.mar	0.57	3
Symphyotrichum novi-belgii	Sym.nov	8.88	16
Taraxacum officinale	Tar.off	1.98	9

Species	Code	% Cover	No. plots
Triglochin maritima	Tri.mar	0.1	1
Trifolium pratense	Tri.pra	4.24	10
Trifolium repens	Tri.rep	0.02	1
Tussilago farfara	Tus.far	0.38	2
Typha angustifolia	Typ.Ang	6.1	6
Typha latifolia	Typ.lat	1.81	1
Unknown Grass	Unk.gra	2.48	4
Unknown seedling	Unk.seed	2.1	5
Vicia sp	Vic.sp	4	6
	Water	2.38	1
	Bare Ground	14.86	18
	Dead Material	3.24	7
	Debris	0.67	2
Unvegetated Area	NO VEG	4.48	11
	Rock	0.67	2
	Species richness	8.4 ± 0.7	
	Halophyte richness	0.8 ± 0.2	
	Halophyte abundance	23.2 ± 6.0	

Habitat Mapping

The 2022 site habitat map is presented in Figure 11 and the proportion of habitat zones presented in Table 6. Areas mapped with dense vegetation cover were classified as dense based on the inability to see bare ground in the imagery (dense vegetation has estimated cover >75%). Areas with sparse cover were generally characterized by clumps of vegetation, with some wetter areas having a base of *Eleocharis palustris*, while bare areas are either entirely bare or with very limited colonization (estimated cover <25%). Bare ground within the classified area was found to be only 13%, which demonstrates the rapid colonization following the DFO Ministerial Order – 87% of the site was vegetated or showing signs of colonization within two growing seasons.

Figure 12 and Figure 13 show plot diversity, wetland score, and dominant species at each station as they relate to habitat mapping. Along Transects 1 and 2, which are low in elevation and close to the tide gate, vegetation was mostly dense with high wetland scores. Species diversity was highest at the upland edge, with halophytic species dominant at most plots. This area was characterized by a mix of early colonizing species and dense monocultures of halophytes. Transects 3 and 4 (~ 1.5 km from tide gate), on the other hand, had large areas of sparse vegetation and bare ground. Where bare ground was not the dominant cover species diversity was generally high, wetland scores low, and dominant species were grasses and ruderals. Transects 5–8 were generally densely vegetated, with high species diversity and a mix of wet meadow and freshwater wetland dominant species. While wetland scores were low on Transects

5 and 6 (3 km from tide gate), they were higher on transects 7–8 (6 km from tide gate), which matches well to lower inundation ratios previously mapped and the distance from the tide gate. These patterns show a gradient along the river with distance from the tide gate—with dominant species transitioning from saltwater to brackish and freshwater species. As elevation increased wetland scores decreased until Transects 7 and 8, where wetland scores were higher despite higher elevations. This may point to changes in hydrology at this location, which is close to the partial "dams" created for Martock's fish habitat offsetting project (Figure 15), or the extent of tidal influence. Examples of typical vegetation cover are shown in Figure 14.

Though data was not collected, early observations of colonization of the mudflat indicated halophytes such as *Sporobolus alterniflorus* to be the most prominent species in the first year of growth. In 2022, while halophytes were still abundant at 23% coverage, freshwater wetland species and weedy ruderals made up the majority of vegetation species found in the study site. The area where the seeding project was carried out remained sparse when compared to other areas, but was showing clear signs of growth in areas where seed was planted (Figure 12). Oblique imagery captured during the drone flight in September show clear growth of grass species in rows as per the planting efforts in May (Figure 16a,b). In some areas natural colonization seemed to also be occurring overtop of seeding, as evident both in aerial imagery and in photos captured on the ground in October (Figure 16c).

Table 6: Classification of habitat zones in Avon River Upstream, 2022.

Class	Area (ha)	% Cover
Bare Ground	34	13%
Water	26	10%
Sparse Cover	59	24%
Dense vegetation	118	47%
Built (Armor and other)	2	1%
Seeding Experiment	13	5%
Total	251	100%

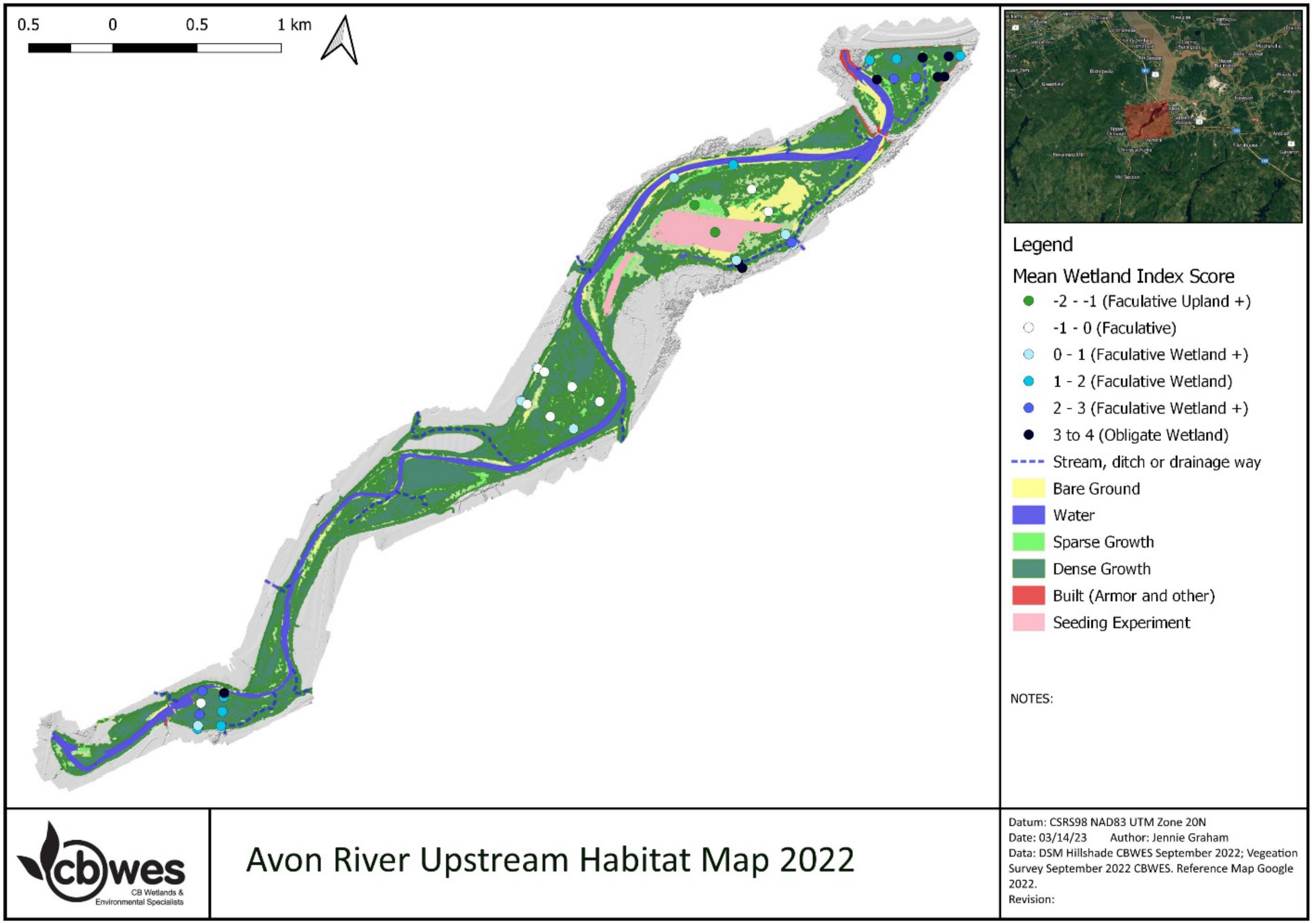

Figure 11: Full site habitat map of the Avon River Upstream, 2022.

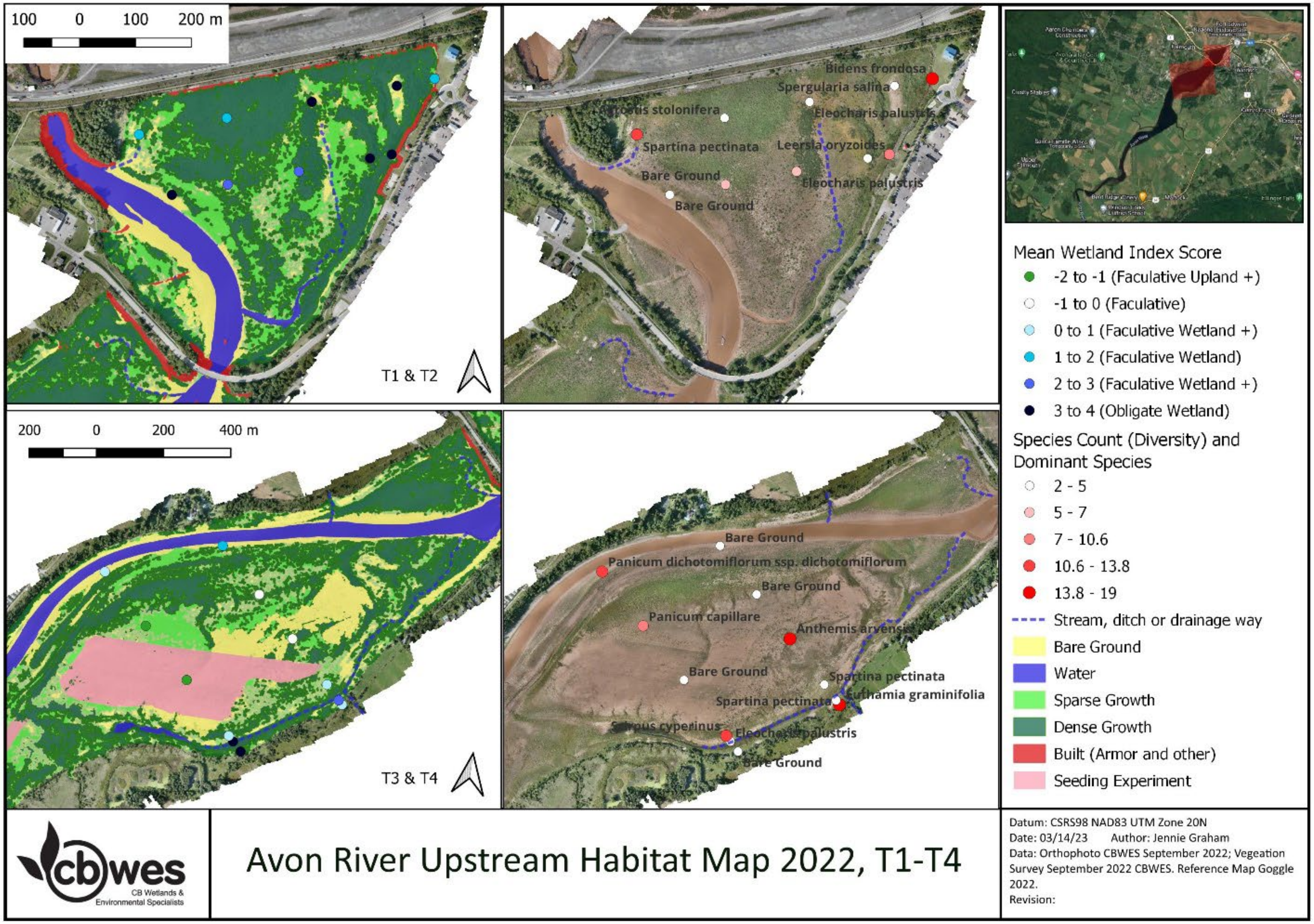

Figure 12: Habitat maps for Transect 1, Transect 2, Transect 3, and Transect 4, 2022.

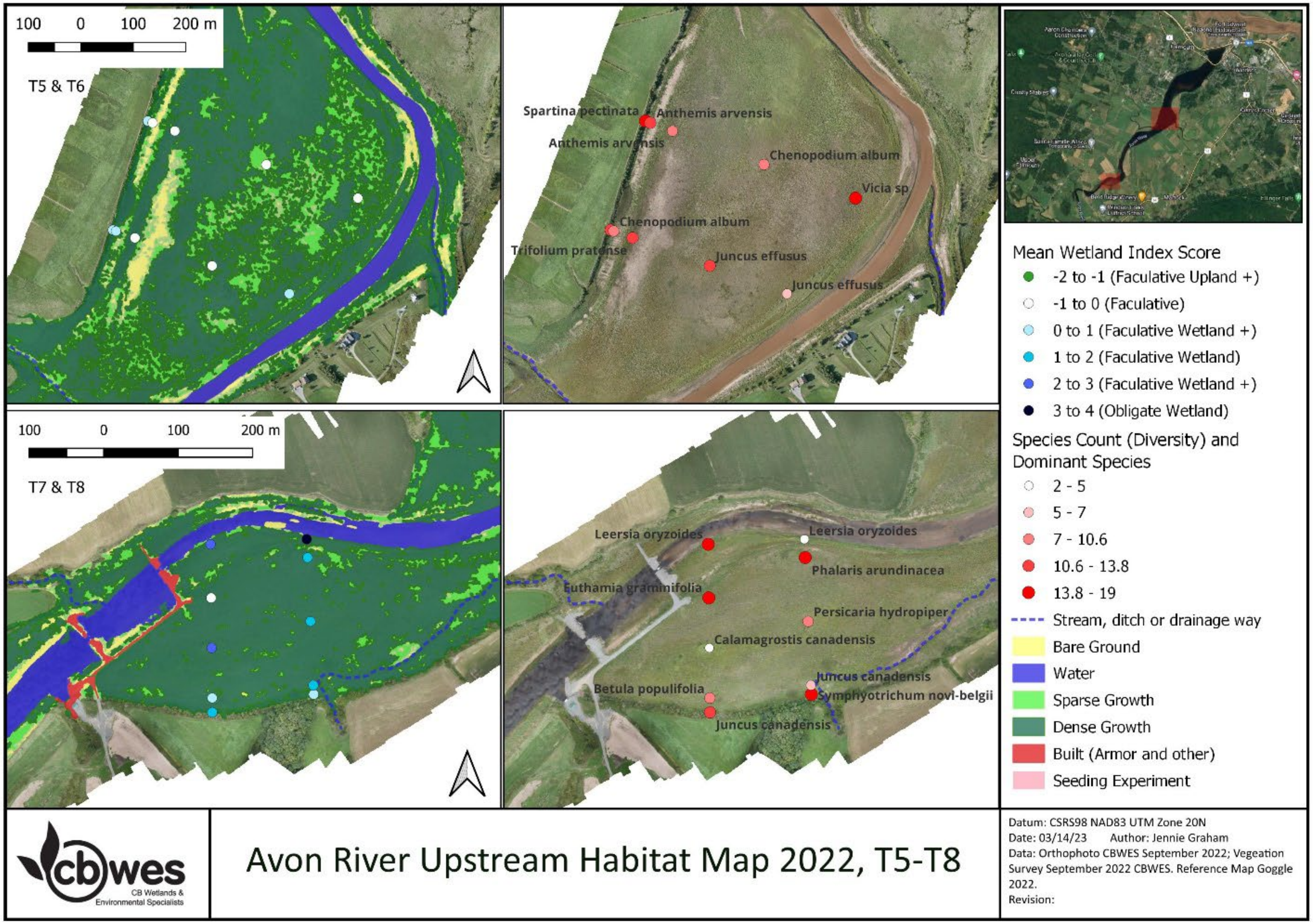

Figure 13: Habitat maps for Transect 5, Transect 6, Transect 7, and Transect 8, 2022.

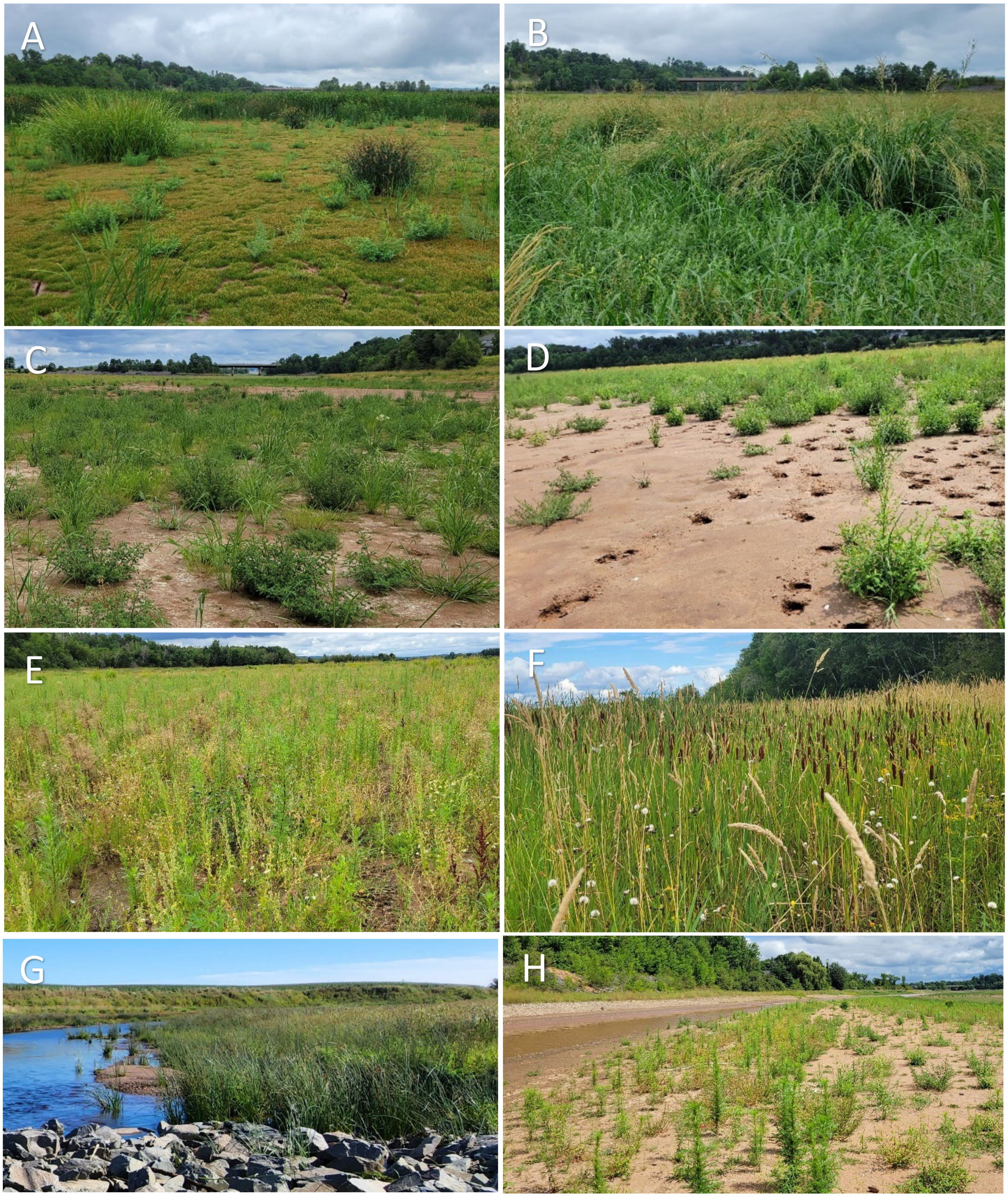

Figure 14: Typical vegetative communities A) *Sporobolus michauxianus* clump with mat of *Eleocharis sp.* B) Dense *Sporobolus michauxianus* C) Sparse grasses and weedy ruderals on sand flat D) Bare ground and sparse *Sueadea* interface E) Dense weedy wet meadow F) Wet Meadow with *Typha sp.* G) Freshwater wetland at river edge H) Sparse ruderals at river edge.

Figure 15: Martock fish habitat offsetting project - partial dam near T7–T8.

Figure 16: The progress of the Windsor Sandbar Seeding Project from A) the planting of the highway seed mix using two tractors and a side-by-side on 13 May 2022, to B) the growth of the planted seeds on 1 September 2022, C) Planting with colonization by weedy ruderals and horse tracks 28 October 2023. Photo A credit: Graeme Matheson (NSDA); photo B credit: Nikki-Marie Lloyd (CMM); photo C: CBWES Inc.

Wildlife Observations

In August, there were horses observed around Transects 3 and 4, and red breasted mergansers were observed in the river. During the 2022 Winter Walk, mergansers, geese, and other waterfowl species were observed where open water was found in the river.

6.0 ECOMORPHODYNAMICS

Ecomorphodynamics refers to the interactions between sediments, intertidal morphology and vegetation colonization. The ecomorphodynamics of the upstream section of the Avon River are highly influenced by the tide gate openings. Since the causeway was completed in 1970, freshwater discharge on the Avon River has been controlled by hydroelectric and storage dams in its upper reaches and by tide gates located in the Avon River Causeway. The tide gates were run on demand from its inception until 1981. This involved manually opening the gates fully on the outgoing tide when the lake level and river were equal. Since 1981, the gates have operated as an automatic system (with manual override) that is designed to maintain Pisiquid Lake (the headpond) at a set elevation. Lake levels would be reduced typically in March to allow for maintenance of gate infrastructure (van Proosdij and Baker, 2007). Gates would also be opened periodically for short periods to accommodate spring movement of gaspereau, otherwise known as alewife and blueback herring (NSTIR, 2017). Sediment-laden tidal waters would move upstream during these periods as well. Between 2016 (Graeme Matheson, NSDA, personal communication, 28 February 2022) and March 2021 the frequency of gate openings and tidal waters flowing upstream for short durations increased as a result of ongoing gate manipulations in order to be in compliance with the terms of the DFO Ministerial Order.

6.1 Methods

Ecomorphodynamic changes were tracked using Sentinel 2 remote sensing satellite imagery between 2019 and December 2021, and are detailed in van Proosdij et al. (2022). The Copernicus Sentinel 2 provides high resolution (10 m) images in the visible and infrared wavelengths and is used to monitor soil, vegetation, water cover and coastal areas. New images are generally available every 5 days and images used in analysis were manually examined to ensure that they were at low tide and had limited cloud cover within the area of the EO Browser (apps.sentinel-hub.com). This report will focus on changes after the Ministerial Order in March 2021. Detailed analysis of gate openings, sediment transport and freshwater discharge is outside of the scope of the current study, however will be required to fully understand any changes in the morphology of the river system upstream of the current causeway.

6.2 Results and Discussion

Based on the interpretation of satellite imagery from April to December 2021, with the re-introduction of partial tidal flow, intertidal flats were rapidly established with one narrow main river thalweg at low tide (Figure 17). Bathymetric analysis reported in van Proosdij et al. (2022) indicate that most sedimentation occurred within the first 450 m upstream section of the river, mostly in Lake Pisiquid. The position of the main river thalweg in the upstream section appears to remain stable from April 2021 to February 2023 (Figure 17, Figure 18, Figure 19). Vegetation and algae growth are evident in the available 26 August 2021 imagery (Figure 17).

A false color composite of the Sentinel-2 imagery using near infrared, red and green bands can be used to assess plant density since plants reflect near infrared and green light while they absorb red. Therefore, areas in red indicate vegetation growth but not the type of vegetation. Figure 20 illustrates the expansion of vegetation between 5 May 2021 and 30 September 2022 and the marked reduction of bare ground. This supports the transect vegetation station findings reported in Section 5. While areas of the large sand bar are slowly being vegetated, bare areas of sand remain. Overall, the system is behaving as expected with even partial re-introduction of tidal flow. Quantifying changes in bathymetry and sediment volume are not possible within this report due to poor weather conditions and lack availability of survey equipment prior to winter.

Figure 17: Copernicus Sentinel-2 satellite imagery (April – October 2021) illustrating sedimentation and evolution of intertidal bar and wetland vegetation after gates opened to allow for fish passage in March 2021. Arrow indicates position of sand bar and site of dust mitigation efforts.

Figure 18: Copernicus Sentinel-2 satellite imagery (December 2021 – July 2022) illustrating sedimentation and evolution of intertidal bar and wetland vegetation after gates opened to allow for fish passage in March 2021.

Figure 19: Copernicus Sentinel-2 satellite imagery (September 2022–February 2023) illustrating sedimentation and evolution of intertidal bar and wetland vegetation after gates opened to allow for fish passage in March 2021.

Figure 20: Copernicus Sentinel-2 imagery displayed as false color bands 8, 4, 3 illustrating vegetation growth on intertidal flats upstream of causeway from 5 May 2021 to 30 September 2022.

7.0 SOILS CHARACTERISTICS

7.1 Methods

Field Methods

Sediment samples (bulk density, organic matter (OM) and grain size) were collected on 28 October 2022, using a stratified random sampling procedure paired with a subset of vegetation sampling plots. Sediment sampling was conducted using a combination of two methods, depending on the dominant sediment composition in each sampling area. Sediment cores were collected conducted at 15 locations and beach scrapes were collected at an additional eight stations in the upstream section of the Avon River. For core stations, two sediment samples were taken. A small (30 mL) sample (for bulk density analysis) was taken using a 60 mL plastic syringe (1” diameter) and a larger sample (for grain size analysis) taken with a metal tube (4” long (~10 cm) and 11⁄2” diameter). Samples were taken by pressing the syringe into the soil to the 30 mL depth indicated on the syringe and removed by cutting around the syringe with a knife before lifting out with a metal trowel. The metal tubes were pressed into the ground until the top of the tube was level with the marsh surface and removed using a knife and/or trowel. The syringes were placed individually into Ziploc bags, sealed, labeled, and transported in a cooler with ice back to the lab where they were placed in a freezer and kept frozen until processing. Some soil compaction does occur during the coring process, but every attempt is made to avoid further compaction of the samples during transport, storage via freezing, and analysis. The metal tubes were capped on both ends using plastic caps and labeled directly. All cores were carefully labeled and sealed using duct tape.

Surface scrapes (top ~2 cm of sand surface) were collected in areas dominated by sand using a trowel. Samples were placed in a ziplock bag, sealed and returned to the In_CoaST lab at Saint Mary’s University.

Laboratory Methods

Cores were processed at the In_CoaST research lab (SMU) for bulk density, water and organic matter content and grain size. Cores were analysed using a Coulter Multisizer 3tm which is based on electrical resistance and is more accurate for the analysis of fine sediments (McCave et al., 2006).

Sample Preparation and Documentation

The sediment cores were thawed before being extruded from their containers. The samples were photographed and split open to see the color, texture, and composition of the core for a qualitative description. This description included the Munsell colour, as the Munsell System allows for direct comparison of soils anywhere in the world. The system has three components: hue (a specific colour), value (lightness and darkness), and chroma (colour intensity) that are arranged in books of colour chips. Values were reported as “Hue Value/Chroma”. For example, 10YR 3/2 represents a hue of 10, YR represents Yellow Red, a value of 3, and a chroma of 2. The top two 2 cm of each half were set aside for loss-on-ignition (LOI) and Coulter Multisizer grain size analysis.

Surface scrape samples were rinsed and dried at 105^{0}C. Samples were mechanically sieved at standard phi intervals from 16 mm to 63 µm with a final sieve of 45 µm. Sieve results were normalized and statistically processed in GRADISTAT (Blott and Pye, 2001) using the Folk and Ward (1957) method. Grain size statistics were derived using GRADISTAT (Blott and Pye, 2001; Figure 21).

Bulk Density

The soil samples were thawed and removed from the syringes. A known volume of sediment was placed in a crucible (known weight) and the weight was recorded. The samples were then oven-dried at 105°C for sixteen hours. The weight of the oven dried sample and the crucible were then recorded again. From this, bulk density was calculated using the following equation:

$$\text{Bulk density } (g \cdot cm^{-3}) = \text{net dry weight } (g) / \text{volume } (cm^3)$$

Organic Content (Using a Loss-on-Ignition Technique)

The sediment cores were thawed and removed from the tubes and the top 2 cm of the core was removed, weighed and placed in a crucible for drying at 105°C for 24 hours to determine water content. Once dried, each sample was weighed and placed in a muffle furnace for two hours at 550°C. Samples were then cooled and weighed again to determine loss of ignition (LOI) of organic material.

Particle Size

To obtain particle size, a portion of the top and bottom 2 cm of each PVC sediment core was separated into size fractions by sieving. Sediments greater than 63 µm were processed at 0.25 phi intervals using standard sieving methods. Fractions finer than 63 µm (silts and clays) were processed using a Coulter Multisizer 3 instrument (or equivalent) to derive disaggregated grain size spectra. Both 30 µm and 200 µm aperture tubes on the Coulter Counter were used and merged in Matlab during analyses. Samples were digested with 30% H_2O_2 prior to processing through the Coulter Counter; therefore, results are of disaggregated inorganic sediments. Milligan and Kranck (1991) elaborate on the methodology of using electroresistance to measure particle size, and McCave et al. (2006) establishes it as more accurate than laser diffraction at measuring fine sediments. The results of the Coulter Counter and the sieving were normalized, and run through GRADISTAT to obtain grain size statistics using the Folk and Ward method (Blott and Pye, 2001).

Grain size		Descriptive terminology			
phi	mm/µm	Udden (1914) and Wentworth (1922)	Friedman and Sanders (1978)	GRADISTAT program	
			Very large boulders		
−11	2048 mm				
			Large boulders	Very large	
−10	1024				
			Medium boulders	Large	
−9	512	Cobbles			
			Small boulders	Medium	Boulders
−8	256				
			Large cobbles	Small	
−7	128				
			Small cobbles	Very small	
−6	64				
			Very coarse pebbles	Very coarse	
−5	32				
			Coarse pebbles	Coarse	
−4	16	Pebbles			
			Medium pebbles	Medium	Gravel
−3	8				
			Fine pebbles	Fine	
−2	4				
		Granules	Very fine pebbles	Very fine	
−1	2				
		Very coarse sand	Very coarse sand	Very coarse	
0	1				
		Coarse sand	Coarse sand	Coarse	
1	500 µm				
		Medium sand	Medium sand	Medium	Sand
2	250				
		Fine sand	Fine sand	Fine	
3	125				
		Very fine sand	Very fine sand	Very fine	
4	63				
			Very coarse silt	Very coarse	
5	31				
			Coarse silt	Coarse	
6	16	Silt			
			Medium silt	Medium	Silt
7	8				
			Fine silt	Fine	
8	4				
			Very fine silt	Very fine	
9	2	Clay			
			Clay	Clay	

Figure 21: Descriptions of common grain size intervals, as modified from prior classifications (Blott and Pye, 2001).

7.2 Results and Discussion

Fifteen of the 19 transect stations upstream of the causeway were dominated by cohesive sediments (containing significant proportion of clays with electrochemical properties that cause sediment particles to bind (stick) together). These stations ranged in elevation from -1.156 to 2.041 m relative to CGVD2013 (Table 8). Cores were quite homogenous with minimal evidence of stratification and minor differences between bottom and top of the core in terms of organic matter content or water content. This is evident in examples of select cores in Figure 22, Figure 23. The Munsell soil descriptions also indicate similarity between the cores. All share the same Hue of 7.5YR (yellow-red) and Value/Chroma ranging from brown (T461 4/4) to very dark brown (T2S5 2/3) (Table 7).

Water content varied from 15% to 51% (Table 8, Figure 23, Figure 26) with highest values in lower lying elevation zones which is not surprising. Organic matter content appears consistent between all the sites (Figure 27), with 13 out of the 16 sample locations ranging from 0% to 15% station and station T3S6 having markedly higher organic matter content with 29% (top) and 25% (bottom) (Figure 27). Because organic matter content is influenced by vegetation and benthic organisms, substrate and elevation play a role in determining organic matter content. Sandy or rocky terrain are less conducive to establishing vegetation and may limit the type and extent of benthic organisms present. Areas that are lower in elevation and experience flooding duration high enough to prevent colonization by vegetation can also have less vegetation and organic matter. While there was no clear trend with station elevation (Figure 24), a possible trend of a slightly higher organic content near the mouth of the system, as compared to the back, may represent an accumulation of organic debris that has flowed downstream and been trapped at the causeway, or diatoms (algae) and other microbial communities on finer marine sediments entering during the incoming tide while the gate remains open (Figure 27). Bulk density for the sites ranged from 0.456 to 1.393 g·cm^{-3} (Table 8, Figure 25, and Figure 28). Bulk density is an indicator of soil compaction and is influenced by grain size. Sandy soils are more prone to high bulk density. The lowest bulk density (0.456 g·cm^{-3}) was recorded at T8S3 which is located furthest up the estuary and is classified as coarse silt (Table 8, Figure 28). The highest value (1.389 g·cm^{-3}) was recorded at T3S6 (Figure 28).

Table 7: Avon upstream 2022 Munsell color identification.

Site	Munsell Color	Munsell Color Description
T1S1	7.5YR 3/4	Dark Brown
T1S3	7.5YR 4/6	Strong Brown
T2S3	7.5YR 3/4	Dark Brown
T2S5	7.5YR 2/3	Very Dark Brown
T3S6	7.5YR 4/6	Strong Brown
T4S6	7.5YR 4/4	Brown
T5S2	7.5YR 4/3	Brown
T5S4	7.5YR 4/6	Strong Brown
T5S4	7.5YR 3/4	Dark Brown
T6S3		
T6S5	7.5YR 4/6	Strong Brown
T7S2	7.5YR 3/3	Dark Brown
T7S4	7.5YR 3/4	Dark Brown

T8S3	7.5YR 3/4	Dark Brown
T8S4	7.5YR 5/6	Strong Brown
T8S5	7.5YR 3/3	Dark Brown

Figure 22: Sample of sediment cores processed in winter 2023.

Table 8: Avon upstream 2022 water content, organic matter content and bulk density for each station where cores were collected. "Top" represents the top 2 cm of the core whereas "Bottom" represents the bottom 2 cm of the core.

Station	Elevation (m)	Water Content (%)		Organic matter content (%)		Dry Bulk Density
		Top	Bottom	Top	Bottom	
T1S1	1.671	24%	38%	3%	7%	1.337
T1S3	-0.291	35%	32%	4%	4%	1.250
T2S3	-0.426	33%	34%	5%	2%	0.960
T2S5	-1.156	38%	38%	5%	5%	1.230
T3S6	0.956	15%	18%	29%	25%	1.389
T4S6	-0.878	36%	35%	5%	4%	1.170
T5S2	-0.358	22%	20%	3%	11%	1.393
T5S4	1.105	30%	27%	6%	5%	1.227
T5S4	0.221	51%	36%	12%	5%	1.227
T6S3	0.384	22%	39%	3%	8%	1.074
T6S5	0.744	37%	44%	5%	7%	1.091
T7S2	1.358	25%	17%	4%	6%	0.801
T7S4	1.822	44%	30%	20%	0%	0.801
T8S3	2.041	35%	50%	8%	14%	0.456
T8S4		24%	17%	5%	3%	1.066
T8S5	-0.58	22%	16%	3%	10%	1.343

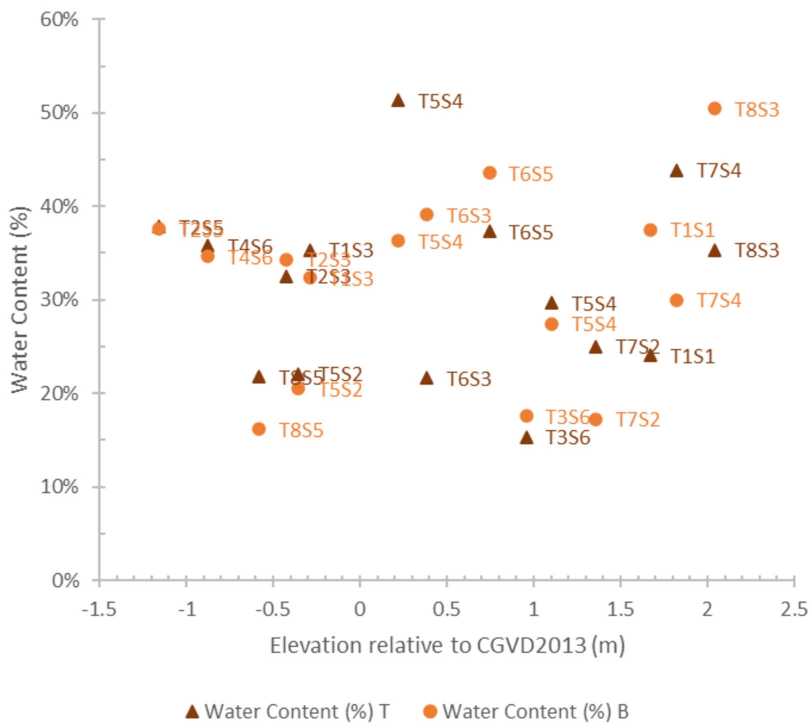

Figure 23: Water content of the core samples taken from the top and bottom 2 cm of each core in percent, versus the elevation in meters.

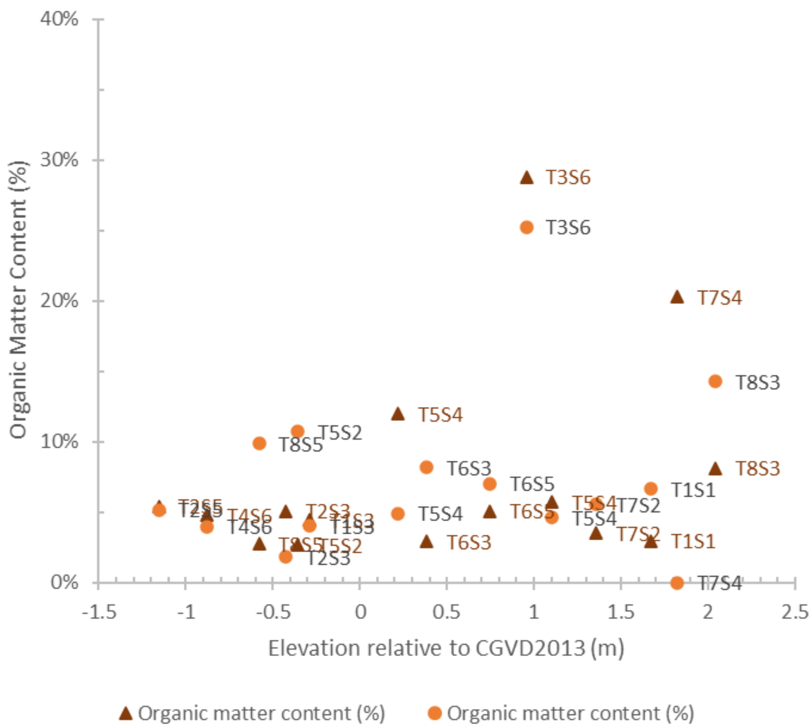

Figure 24: Organic matter content of the samples taken from the top and bottom 2 cm of each core in percent, versus the elevation in meters.

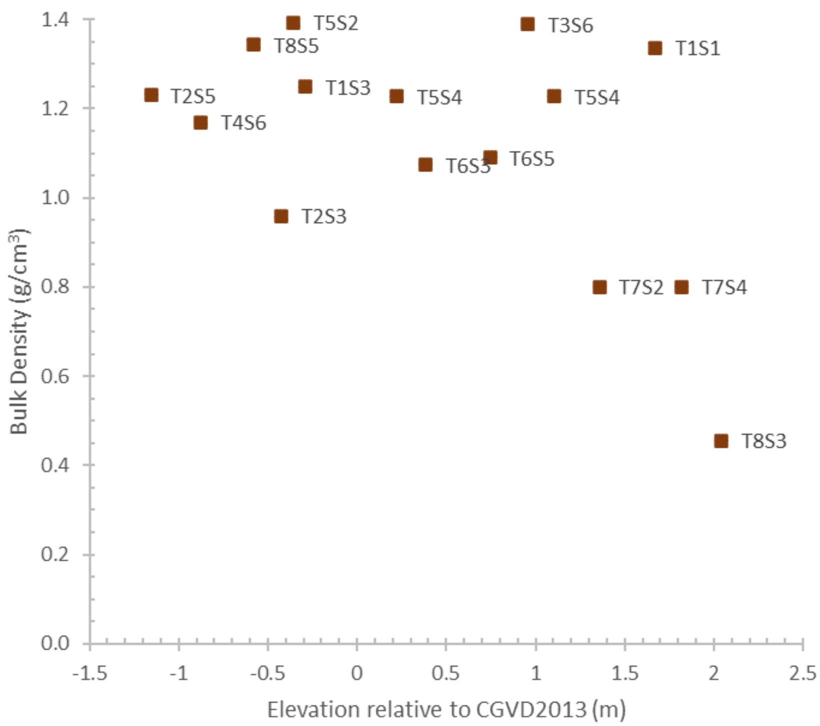

Figure 25: Dry bulk density of each syringe sample at core stations upstream of the Windsor causeway.

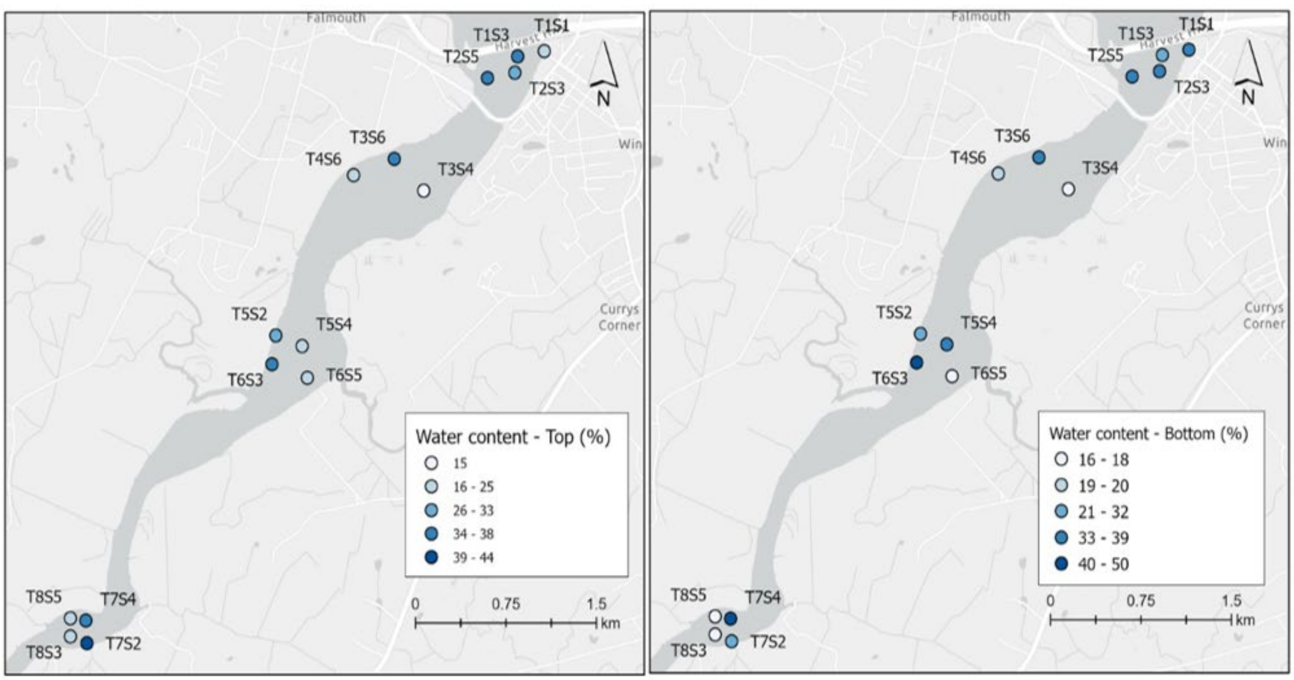

Figure 26: Map of stations' water content from the tops and bottom of Avon River upstream sediment cores, 2022.

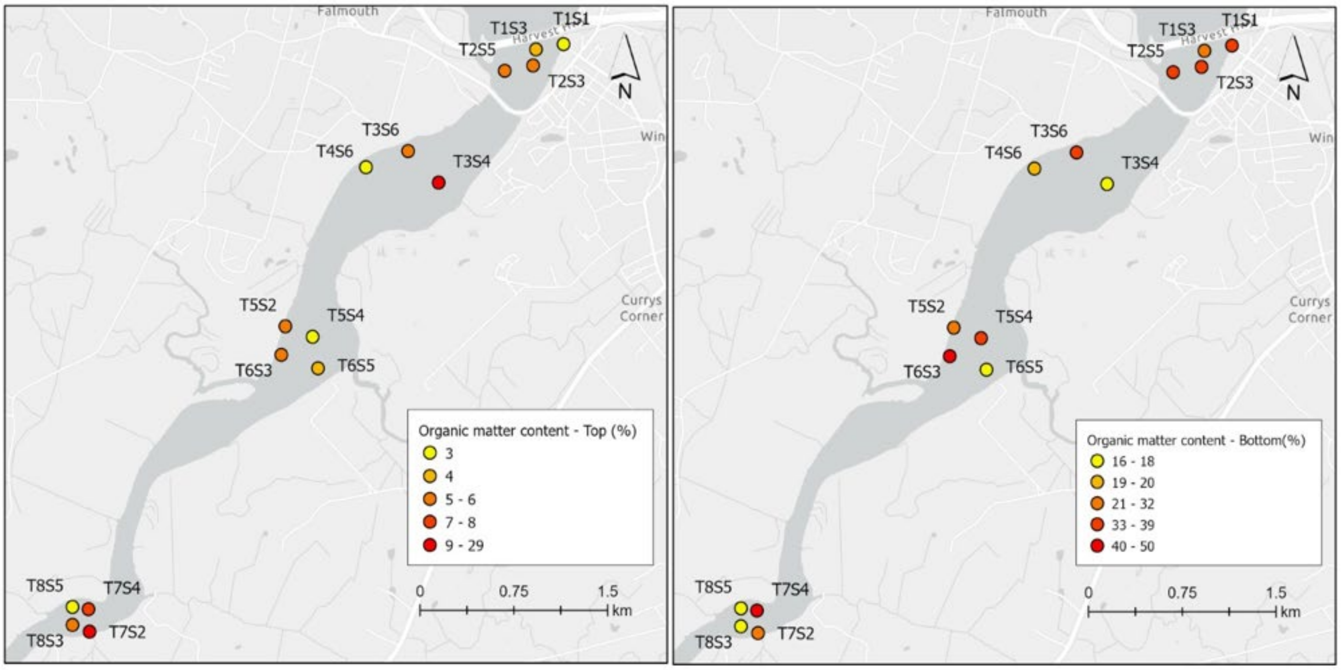

Figure 27: Map of stations' organic matter content (%) for tops and bottom of cores collected at Avon River upstream, 2022.

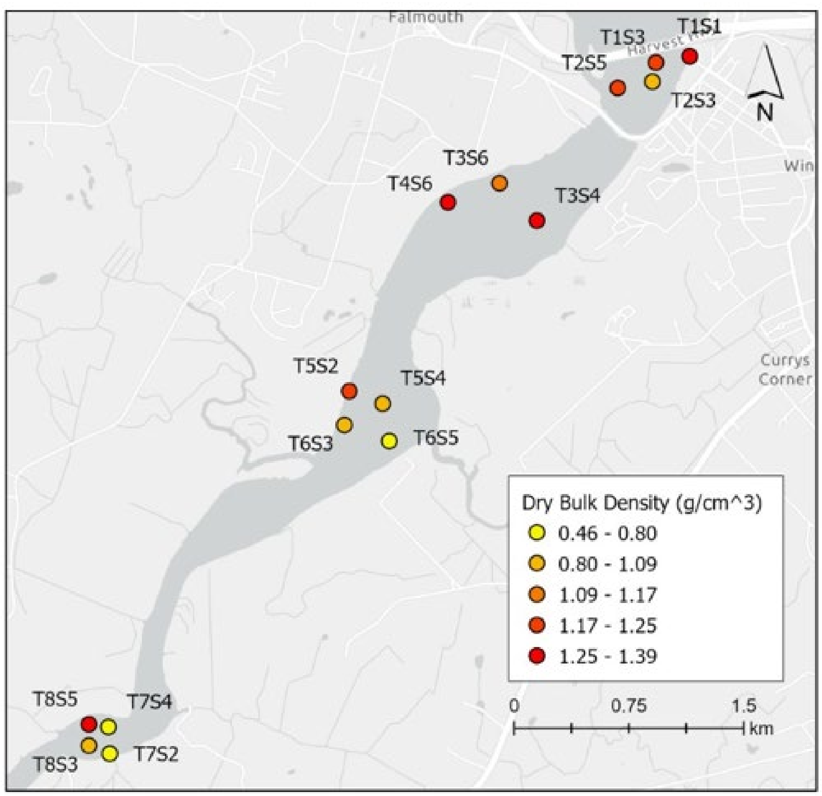

Figure 28: Map of stations' bulk density (g/cm^3) of syringe cores collected at on River upstream, 2022.

All of the cores in the medium (T4S6, T5S2, T6S5) and coarse silt (T1S3, T5S4, T7S2, T7S4, T8S3, T8S4) categories were texturally classified as mud (Table 9). The smallest mean grain size was 9.64 µm at T4S6 and largest 18.16 µm T8S4 (Table 9). These grain sizes are consistent with mean grain sizes recorded downstream in previous studies (van Proosdij et al., 2020) suggesting that this material was brought in by the tides. However, medium and coarse silt were also reported upstream in van Proosdij et al., 2020, and therefore cannot be attributed solely to the new gate openings. The eight surface scrape samples collected at the Avon River site in 2022 were within the fine sand category, which can be seen in Table 9. These samples were collected primarily on the main "Windsor Sandbar" which has some of the highest elevation points on the site and was the site of 'dust mitigation' efforts (The Seeding Project; Figure 2, Figure 17). The textural groups of the samples ranged from muddy sand to slightly gravelly sand. The mean grain sizes ranged from 164 µm to 219 µm. Majority of the samples were moderately well sorted with the exception of BE_S2 /and BW_S3 which were poorly sorted, and T4S3 which was well sorted.

Table 9: The category, textural group, and mean grain size of sediment samples collected at Avon River upstream, 2022 processed using a Coulter Counter Multisizer 3, 2022. Sand samples were processed using a sediment sieve.

Station	Sample Type	Category	Textural Group	Mean grain size (µm)
T1S3	Sediment Core	Coarse Silt	Mud	15.06
T3S4	Sand Sample	Fine Sand	Sand	172.0
T4S3	Sand Sample	Fine Sand	Sand	171.4
T4S4	Sand Sample	Fine Sand	Sand	164.4
T4S5	Sand Sample	Fine Sand	Sand	175.4
T4S6	Sediment Core	Medium Silt	Mud	9.64
T5S2	Sediment Core	Medium Silt	Mud	13.73
T5S4	Sediment Core	Coarse Silt	Mud	17.96
T6S5	Sediment Core	Medium Silt	Mud	17.45
T7S2	Sediment Core	Coarse Silt	Mud	16.69
T7S4	Sediment Core	Coarse Silt	Mud	17.41
T8S3	Sediment Core	Coarse Silt	Mud	15.00
T8S4	Sediment Core	Coarse Silt	Mud	18.16
BE_S2	Sand Sample	Fine Sand	Slightly gravelly sand	219.7
BW_S1	Sand Sample	Fine Sand	Muddy sand	149.7
BW_S3	Sand Sample	Fine Sand	Slightly gravelly sand	188.3
BW_S4	Sand Sample	Fine Sand	Slightly gravelly sand	171.0

8.0 WINTER CONDITIONS

Observations of site conditions during winter visual assessments provides context for spring observations and insight into winter processes happening at the sites. Large ice chunks, variability in snow and ice cover, and winter storm debris are examples of observations that can be made during a winter visit that may explain unusual features and patterns observed in the spring. Winter conditions play a key role in channel morphology due to ice transport and the role of storms in sediment transport. Variability in winter conditions over years can also help to explain year to year sediment, vegetation, or geospatial differences at the sites.

8.1 Methods

Structured walks involved traversing the perimeter of the site with landscape photographs taken from the first station toward the Avon River at each transect. Key features such as channels, the tide gate structure, causeway edge, dykes, significant ice formations, areas of erosion or deposition, and other features of note were also photographed. Due to the access safety concerns, only Transect 1, 2, 3, and 4 were documented for the winter walk. It is not anticipated that Transects 5, 6, 7, and 8 would have provide significantly different information than the first four transects.

8.2 Results

A structured winter walk was conducted on 9 February 2023 at AVUS in order to document and evaluate winter conditions at the site. The day of the walk had clear skies with temperature of -5°C. Average temperatures recorded at the Kentville CDA CS weather station[6] for the 2022/23 winter season were below freezing for December (-2.2°C), January (-0.4°C), and until from February 1 to 9 (-7.7°C). There was no snow cover in December, approximately six days of snow cover in January, and patches of snow cover ranging from 0–8 cm depth in February. The first nine days of February had temperatures ranging from 4.7°C to -25.5°C, an enormous and atypical range in temperatures for February in area.

During the walk there was partial snow and ice coverage (Figure 29). Broken ice slabs were visible along the banks of the Avon River upstream of the tide gates (Figure 30).

[6] https://climate.weather.gc.ca/historical_data/search_historic_data_e.html

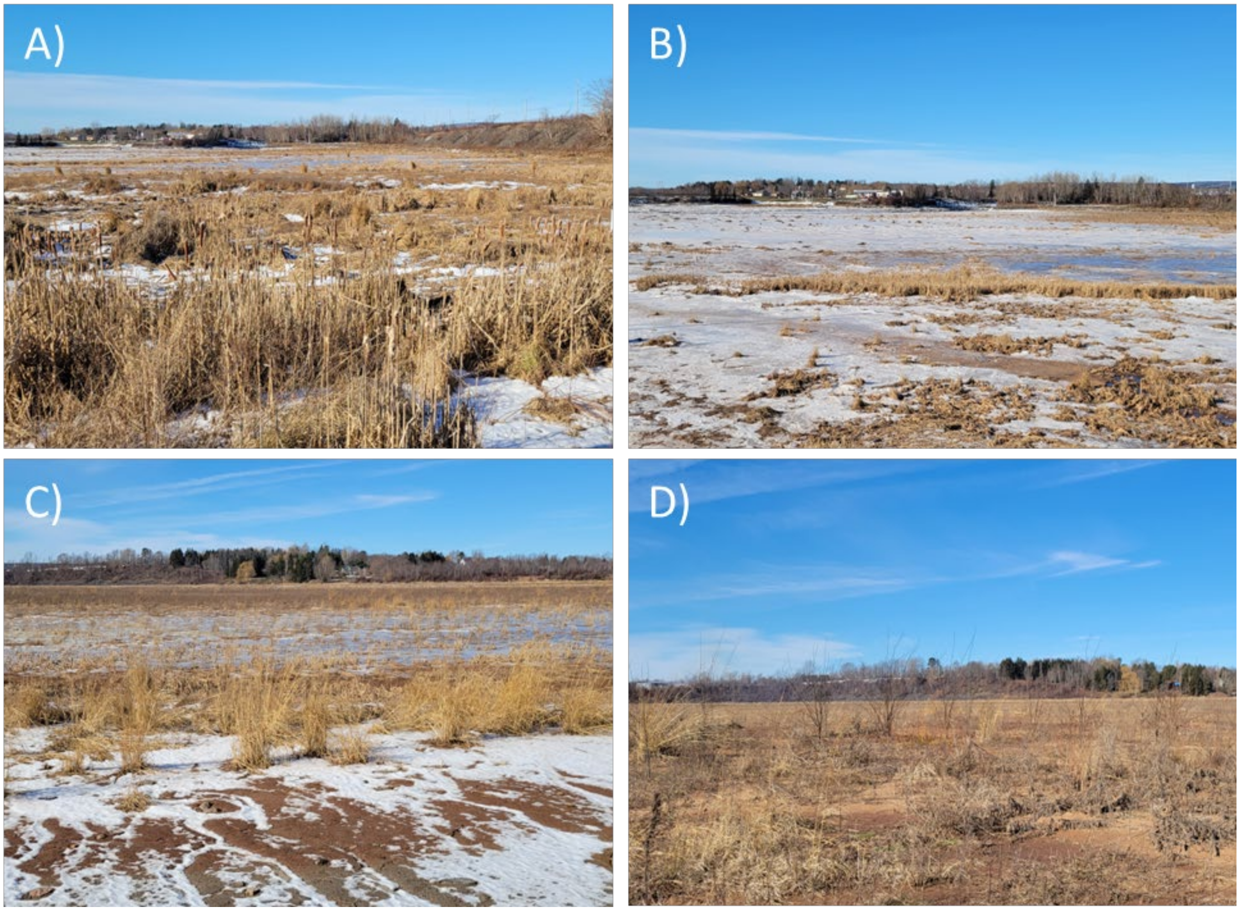

Figure 29: Landscape photographs along Transect 1–4 being monitored at the Avon River upstream the Causeway: A) Transect 1; B) Transect 2; C) Transect 3; D) Transect 4. Photos taken 9 February 2023.

Figure 30: Ice slabs on the banks of the Avon River, 9 February 2023.

9.0 SUMMARY AND CONCLUSIONS

This report provides documentation of the conditions existing upstream of the Avon River Causeway during modified gate operations in the summer of 2022. They present a significant change in the ecological condition of the river following the implementation of the DFO Ministerial Order requiring fish passage to the area above the causeway. With the headpond (Lake Pisiquid) drawn down and the river allowed to flow in a "more natural" way—in the sense that there is now some bidirectional flow and saltwater has been re-introduced to a system that had been anthropogenically made freshwater— the hydrology remains primarily influenced by human activities. This is particularly apparent when looking at the highest upstream water level of the year, and was approximately 5x higher than the average high upstream water level caused primarily by NS Power spilling the upstream hydroelectric dam. This also coincided with a significant precipitation event (27.8 mm).

At the time of the study, vegetation had colonized 87% of the exposed sand and mudflats, areas which had been permanently inundated while the head pond was maintained. The vegetation communities were primarily wetland and wet-meadow types, with halophytes comprising 23% of the species identified and their dominance decreasing with distance from the tide gate. Elevation, hydroperiod and soils played a key role in the distribution and density of vegetation, with the "Windsor Sandbar" remaining sparsely vegetated while most other areas have become densely vegetated. The Seeding Project carried out in May of 2022 resulted in growth of new vegetation that was clearly visible both from the air and the ground, reducing bare ground area and presumably likewise reducing the mobilization of fine sediments. Soil characteristics are still showing influence from the previously established freshwater system but are now shifting towards more estuarine characteristics with increasing contributions of fines (at least until June 2023 when EMO Minister John Lohr invoked an emergency order to close the tide gates).

Operations of the gate since the DFO Ministerial Order in March of 2021 had allowed for the development of dynamic wetland habitat upstream of the causeway, that ranges from salt through brackish to freshwater conditions. It should be noted that further changes in operations will present further disruption in the ecosystem and could once again shift these communities (as we have seen since 1 June 2023). Increased tidal inundation may result in increased dominance of halophytes in some areas and creation of new mudflat, while decreased tidal flooding could have the opposite effect (decreased halophytic dominance). Further, prolonged flooding is likely to lead to a rapid dieback of the re-established vegetation communities with implications to future soil formation in the river floodplain, and future habitat conditions, productivity and biodiversity.

10.0 REFERENCES

Audubon Society. (1993). The Audubon Society Field Guide to North American Fishes, Whales & Dolphins. Random House of Canada Ltd., Toronto, ON.

Baas, J.H., Best, J.L., and Peakall, J. (2015). Predicting bedforms and primary current stratification in cohesive mixtures of mud and sand. *J. of the Geo. Soc.* doi:10.1144/jgs2015-024

Bales, RC. (2015). Hydrology, Floods and Droughts | Overview, Editor(s): Gerald R. North, John Pyle, Fuqing Zhang, Encyclopedia of Atmospheric Sciences (Second Edition), Academic Press, Pages 180-184, ISBN 9780123822253, https://doi.org/10.1016/B978-0-12-382225-3.00166-3.

Bowron, T.; Neatt, N.; van Proosdij, D. and J. Lundholm. 2012. Chapter 14: Salt Marsh Restoration in Atlantic Canada In Restoring Tidal Flow to Salt Marshes: A Synthesis of Science and Management." Burdick and Roman (eds). Island Press. p. 191-210.Daborn, G.R.; van Proosdij, D. and M. Brylinsky. (2003). Environmental Implications of Expanding the Windsor Causeway (Part One). Report prepared for Nova Scotia Department of Transportation Contract # 02-00026. Acadia Centre for Estuarine Research Publication No. 72. 15 pp.

Dionne, M., F.T. Short, and D.M Burdick. (1999). Fish Utilization of Restored, Created and Reference Salt-Marsh Habitat in the Gulf of Maine. American Fisheries Society Symposium 22:384-404.

Gerwing, T.G., Davies, M.M., Clements, J., Flores, A-M., Thomson, H.M., Nelson, K.R., Kushneryk, K., Brouard-John, E.K., Harvey, B., Plate, E. (2020). Do you want to breach an embankment? Synthesis of the literature and practical considerations for breaching of tidally influenced causeways and dikes. *Estuarine, Coastal and Shelf Science*, 245. https://doi.org/10.1016/j.ecss.2020.107024.

Gerwing, T.G., Hamilton, D.J., Barbeau, M.A., Haralampides, K., Yamazaki, G. (2017). Short-term response of a downstream marine system to the partial opening of a tidal-river causeway. *Estuaries and Coasts* 40:717-725. http://www.jstor.org/stable/44857846.

Global Programme of Action Coalition (GPAC). (1999). Regional Standards to Identify and Evaluate Tidal Wetland Restoration in the Gulf of Maine. A GPAC Workshop Report. Edited by Hilary Neckles and Michele Dionne. Wells National Estuarine Research Reserve, June 2-3, 1999. Wells, ME.

Graff, L. and J. Middleton. (2002). Wetlands and Fish: Catch the Link. National Oceanic and Atmospheric Administration (NOAA), National Marine Fisheries Service. Maryland.

Graham, J., Bowron, T.M., van Proodij, D., Baker, G., Ellis, K. (2018). Avon River aboiteau and causeway upgrades: Pre-construction monitoring of the Avon River estuary. Prepared for Nova Scotia Department of Transportation and Infrastructure Renewal. CBWES Publication No. 55. Halifax, NS.

Hugenholtz, C., Brown, O., Walker, J., Barchyn, T., Nesbit, P., Kucharczyk, M., and Myshak, S. (2016). Spatial Accuracy of UAV-Derived Orthoimagery and Topography: Comparing Photogrammetric Models Processed with Direct Geo-Referencing and Ground Control Point. *Geomatica* 70(1). https://doi.org/10.5623/cig2016-102.

Kickbush, J., Graham, J., Bowron, T.M., van Proosdij, D., Lewis, Ellis, K. 2023. Avon River Aboiteau and Causeway Phase 1 Upgrades: 2022 Season Post-construction Monitoring of the Windsor and Elderkin Salt Marshes. Prepared for Nova Scotia Department of Public Works. CBWES Publication No. 79. Halifax, NS.

Kineke, G.C. and Milligan, T.G. (2015). Fluid mud in energetic systems: Flumes II. Annual Report. Prepared by Boston College. Available from https://apps.dtic.mil/sti/citations/ADA514891

Kwak, T. and J.B. Zedler. (1997). Food Web Analysis of Southern California Coastal Wetlands Using Multiple Stable Isotopes. *Oecologia* 110: 262-277.

James, M.R. and Robson, S. (2014). Mitigating systematic error in topographic models derived from UAV and ground-based image networks. *Earth Surface Processes and Landforms* 39(10). https://doi.org/10.1002/esp.3609.

Lloyd, N-M. 2022. Dust Mitigation on the Avon River: Project Summary Report. Prepared for TransCoastal Adaptations: Centre for Nature-Based Solutions, Saint Mary's University. Confederacy of Mainland Mi'Kmaq. Millbrook, NS.

Mitsch, W.J. and J.G. Gosselink. (1986). Wetlands. Van Nostrand Reinhold Co., New York, N.Y.

Neckles, H. and M. Dionne. (eds.). (2000). Regional Standards to Identify and Evaluate Tidal Wetland Restoration in the Gulf of Maine. A GPAC Workshop. Wells National Estuarine Research Reserve, Wells, ME.

Nova Scotia Transportation and Infrastructure Renewal (NSTIR). (2017). Restoration of Nova Scotian Salt Marshes. Retrieved from: https://novascotia.ca/tran/works/enviroservices/enviroSaltMarsh.asp. Last updated: December 1, 2017.

Raczynski, R. J. (2017). 'Accuracy analysis of products obtained from UAV-borne photogrammetry influenced by various flight parameters', (Engineering Masters), Norwegian University of Science and Technology, Norwegian University of Science and Technology.

Roman, C.T., K.B. Raposa, S.C. Adamowicz, M-J. James-Pirri, and J.G. Catena. (2002). Quantifying Vegetation and Nekton Response to Tidal Restoration of a New England Salt Marsh. *Restoration Ecology* 10(3): 450-460.

Ross, M.A. and Mehta. (1989). On the mechanics of lutoclines and fluid mud. *J. Coast. Res., Spec. Issue,* 5, 51-61.

Scott, W.B. and M.G. Scott. (1988). Atlantic Fishes of Canada. *Can. Bull. Fish. Aquat*.

Tonkin, T.N. and Midgley, N.G. (2016). Ground-Control Networks for Image Based Surface Reconstruction: An Investigation of Optimum Survey Designs Using UAV Derived Imagery and Structure-from-Motion Photogrammetry. Remote Sensing 8(9), 786, https://doi.org/10.3390/rs8090786.

van Proosdij, D., Daborn., G.R. and M. Brylinsky. (2004). Environmental Implications of Expanding the Windsor Causeway (Part Two): Comparison of 4 and 6 Lane Options. Report prepared for Nova Scotia Department of Transportation Contract # 02-00026. Acadia Centre for Estuarine Research Publication No. 75. 17 pp.

van Proosdij, D. (2005). Monitoring Seasonal Changes in Surface Elevation in Intertidal Environments near the Windsor Causeway. Final report prepared for the Nova Scotia Department of Transportation 22 pp.

van Proosdij, D; Bambrick, J. and G. Baker. (2006a). Spatial and Temporal Variations in the Intertidal Geomorphology of the Avon River Estuary. Final report prepared for the Nova Scotia Department of Transportation. 82 pp.

van Proosdij, D. and S., Townsend. (2006). Spatial and Temporal Patterns of Salt Marsh Colonization Following Causeway Construction in the Bay of Fundy. *Journal of Coastal Research*, SI 39:1858-1862, ISSN 0749-0208.

van Proosdij, D.; Ollerhead, J. and R.G.D. Davidson-Arnott. (2006b). Seasonal and annual variations in the sediment mass balance of a macro-tidal salt marsh. *Marine Geology* 225:103-127.

van Proosdij, D. and G. Baker. (2007). Intertidal Morphodynamics of the Avon River Estuary. Final report prepared for the Nova Scotia Department of Transportation. 186 pp.

van Proosdij, D., Milligan, T., Bugden, G. and C. Butler. (2009). A Tale of Two Macro Tidal Estuaries: Differential Morphodynamic Response of the Intertidal Zone to Causeway Construction. *Journal of Coastal Research* SI 56: 772-776. ISBN 0749-0258.

van Proosdij, D. and Bowron, T.M. (2017). Contemporary Morphodynamics of the Avon River Estuary and Recommended Monitoring Plan Before and After Highway 101 Twinning – Final Report. Prepared for Nova Scotia Department of Transportation. 47 pp.

van Proosdij, D., Baker, G., Poirier, E., Aykol, R., Lewis, S. (2020). Sediment Dynamics of the Avon Tide Gate Channel: Implications for Modelling and Aboiteau Design. Final report prepared for CBCL Ltd Consulting Engineers, sub-contract 170146.00 78p.

van Proosdij, D., Baker, G.. Poirier, E., and T. Bowron (2022). Examination of the Morphodynamics of the Upstream Portion of the Avon River. Prepared for Mi'kmaw Conservation Group, Confederacy of Mainland Mi'kmaq. 22 pp.

Westoby, M.J., Brasinton, J., Glasseu, N.F., Hambrey, M.J. and J.M. Reynolds. (2012). 'Structure-from-motion' photogrammetry: a low cost, effective tool for geoscience applications. *Geomorphology*, 179:300-314.

APPENDIX A

Table 1: AVUS plot wetland status indicator values. Values calculated as the average wetland indicator value across all species in a plot.

Station	Elevation (m)	Average wetland indicator value
AVUS_T1S1	1.671	1.3
AVUS_T1S2	0.821	4.0
AVUS_T1S3	-0.291	4.0
AVUS_T1S4	0.12	1.8
AVUS_T1S5	-0.112	1.9
AVUS_T2S1	-0.196	3.1
AVUS_T2S2	-0.192	4.0
AVUS_T2S3	-0.426	2.5
AVUS_T2S4	-0.501	2.5
AVUS_T2S5	-1.156	4.0
AVUS_T3S1	4.198	0.1
AVUS_T3S2	1.012	3.0
AVUS_T3S3	0.116	1.0
AVUS_T3S4	0.956	0.0
AVUS_T3S5	0.265	-0.7
AVUS_T3S6	-0.878	1.3
AVUS_T4S1	1.546	3.5
AVUS_T4S2	-0.19	4.0
AVUS_T4S3	0.534	0.7
AVUS_T4S4	1.195	-1.3
AVUS_T4S5	0.92	-1.3
AVUS_T4S6	-0.358	0.5
AVUS_T5S1	1.44	0.7
AVUS_T5S2	1.105	-0.4
AVUS_T5S3	0.295	-0.3
AVUS_T5S4	0.221	-0.4
AVUS_T5S5	0.554	-0.1
AVUS_T6S1	1.65	0.9
AVUS_T6S2	1.313	0.6
AVUS_T6S3	0.384	-0.4
AVUS_T6S4	0.731	-0.3
AVUS_T6S5	0.744	0.9
AVUS_T7S1	1.42	0.5

Station	Elevation (m)	Average wetland indicator value
AVUS_T7S2	1.358	1.1
AVUS_T7S3	1.879	1.6
AVUS_T7S4	1.822	1.3
AVUS_T7S5	-0.478	3.2
AVUS_T8S1	1.821	1.8
AVUS_T8S2	1.71	0.6
AVUS_T8S3	2.041	2.5
AVUS_T8S4	1.652	-0.1
AVUS_T8S5	-0.58	2.1

APPENDIX B: SEDIMENT SAMPLE STATISTICS

SAMPLE STATISTICS

SIEVING ERROR: 0.1%

SAMPLE IDENTITY: **AUUS T453**

ANALYST & DATE: Leila Rashid, 28/10/2022

SAMPLE TYPE: Unimodal, Well Sorted

TEXTURAL GROUP: Sand

SEDIMENT NAME: Well Sorted Fine Sand

	μm	ϕ
MODE 1:	187.5	2.500
MODE 2:		
MODE 3:		
D_{10}:	117.1	2.078
MEDIAN or D_{50}:	171.4	2.545
D_{90}:	236.8	3.094
(D_{90} / D_{10}):	2.022	1.489
(D_{90} - D_{10}):	119.7	1.016
(D_{75} / D_{25}):	1.498	1.259
(D_{75} - D_{25}):	69.77	0.583

GRAIN SIZE DISTRIBUTION

GRAVEL:	0.0%	COARSE SAND:	0.3%
SAND:	99.3%	MEDIUM SAND:	3.0%
MUD:	0.7%	FINE SAND:	85.7%
		V FINE SAND:	10.2%
V COARSE GRAVEL:	0.0%	V COARSE SILT:	0.4%
COARSE GRAVEL:	0.0%	COARSE SILT:	0.1%
MEDIUM GRAVEL:	0.0%	MEDIUM SILT:	0.1%
FINE GRAVEL:	0.0%	FINE SILT:	0.1%
V FINE GRAVEL:	0.0%	V FINE SILT:	0.1%
V COARSE SAND:	0.0%	CLAY:	0.1%

	METHOD OF MOMENTS			FOLK & WARD METHOD		
	Arithmetic μm	Geometric μm	Logarithmic ϕ	Geometric μm	Logarithmic ϕ	Description
MEAN ($\bar{x}$):	184.3	166.2	2.589	171.4	2.545	Fine Sand
SORTING (σ):	57.13	1.391	0.476	1.351	0.434	Well Sorted
SKEWNESS (Sk):	4.900	-3.464	3.464	-0.163	0.163	Fine Skewed
KURTOSIS (K):	64.87	35.77	35.77	1.094	1.094	Mesokurtic

GRAIN SIZE DISTRIBUTION

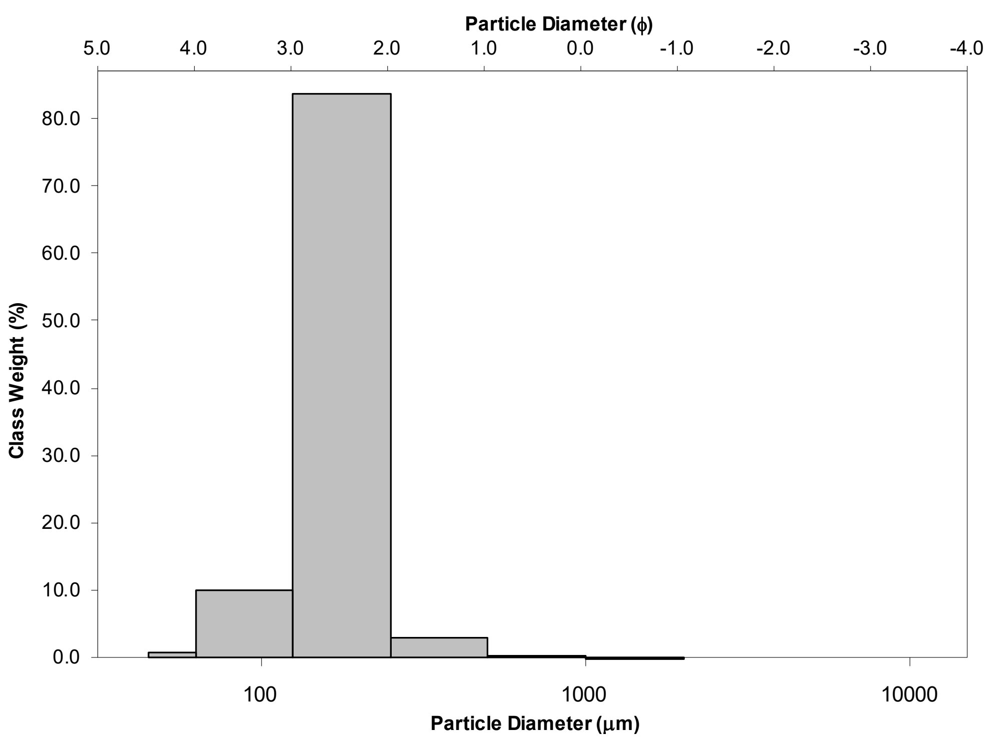

SIEVING ERROR: 0.1%

SAMPLE STATISTICS

SAMPLE IDENTITY: **AUUS T454** ANALYST & DATE: Leila Rashid, 28/10/2022

SAMPLE TYPE: Unimodal, Moderately Well Sorted TEXTURAL GROUP: Sand

SEDIMENT NAME: Moderately Well Sorted Fine Sand

	μm	φ
MODE 1:	187.5	2.500
MODE 2:		
MODE 3:		
D_{10}:	84.71	1.921
MEDIAN or D_{50}:	169.8	2.558
D_{90}:	264.0	3.561
(D_{90} / D_{10}):	3.117	1.854
$(D_{90} - D_{10})$:	179.3	1.640
(D_{75} / D_{25}):	1.634	1.322
$(D_{75} - D_{25})$:	84.25	0.709

GRAIN SIZE DISTRIBUTION

GRAVEL:	0.0%	COARSE SAND:	2.5%
SAND:	96.7%	MEDIUM SAND:	8.0%
MUD:	3.3%	FINE SAND:	70.6%
		V FINE SAND:	15.5%
V COARSE GRAVEL:	0.0%	V COARSE SILT:	1.2%
COARSE GRAVEL:	0.0%	COARSE SILT:	0.4%
MEDIUM GRAVEL:	0.0%	MEDIUM SILT:	0.4%
FINE GRAVEL:	0.0%	FINE SILT:	0.4%
V FINE GRAVEL:	0.0%	V FINE SILT:	0.4%
V COARSE SAND:	0.1%	CLAY:	0.4%

	METHOD OF MOMENTS			FOLK & WARD METHOD		
	Arithmetic μm	Geometric μm	Logarithmic φ	Geometric μm	Logarithmic φ	Description
MEAN ($\bar{x}$):	198.2	159.8	2.646	164.4	2.604	Fine Sand
SORTING (σ):	119.4	1.899	0.926	1.587	0.667	Moderately Well Sorted
SKEWNESS (Sk):	3.639	-2.418	2.418	-0.075	0.075	Symmetrical
KURTOSIS (K):	23.98	14.85	14.85	1.492	1.492	Leptokurtic

GRAIN SIZE DISTRIBUTION

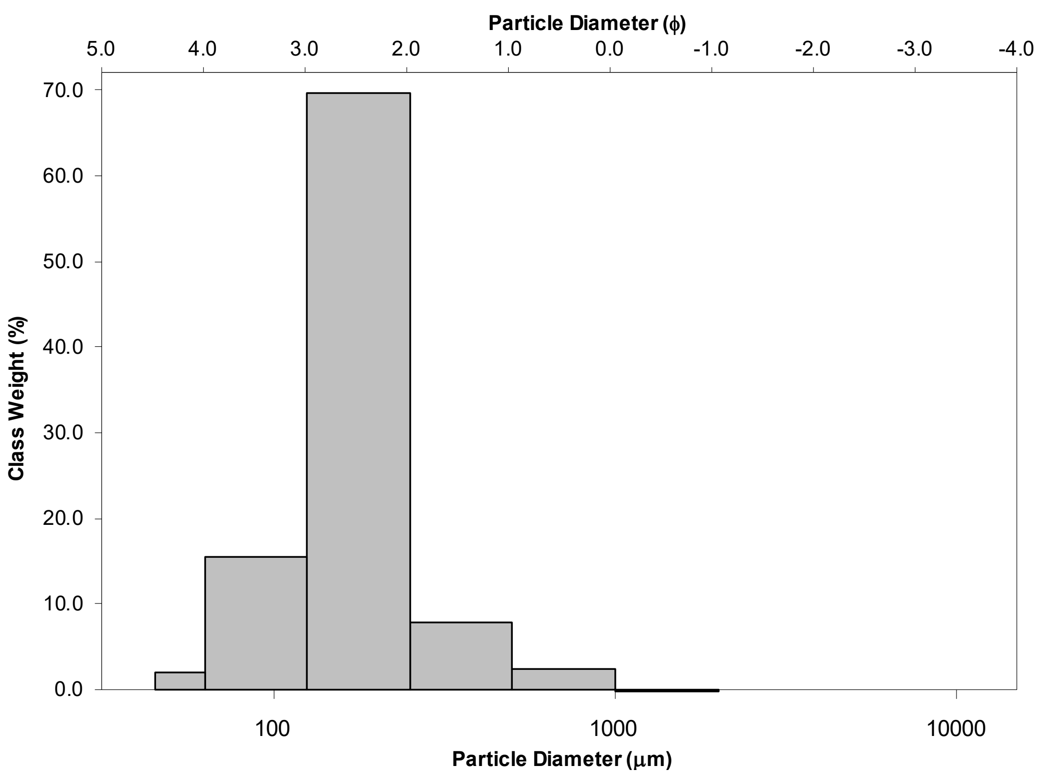

SAMPLE STATISTICS

SIEVING ERROR: 0.1%

SAMPLE IDENTITY: **AUUS T455** ANALYST & DATE: Leila Rashid, 28/10/2022

SAMPLE TYPE: Unimodal, Moderately Well Sorted TEXTURAL GROUP: Sand

SEDIMENT NAME: Moderately Well Sorted Fine Sand

	μm	ϕ
MODE 1:	187.5	2.500
MODE 2:		
MODE 3:		
D_{10}:	112.3	2.003
MEDIAN or D_{50}:	175.4	2.511
D_{90}:	249.4	3.155
(D_{90} / D_{10}):	2.221	1.575
(D_{90} - D_{10}):	137.2	1.152
(D_{75} / D_{25}):	1.552	1.289
(D_{75} - D_{25}):	77.79	0.635

GRAIN SIZE DISTRIBUTION

GRAVEL:	0.0%	COARSE SAND:	3.1%
SAND:	97.9%	MEDIUM SAND:	6.5%
MUD:	2.1%	FINE SAND:	78.8%
		V FINE SAND:	9.4%
V COARSE GRAVEL:	0.0%	V COARSE SILT:	1.1%
COARSE GRAVEL:	0.0%	COARSE SILT:	0.2%
MEDIUM GRAVEL:	0.0%	MEDIUM SILT:	0.2%
FINE GRAVEL:	0.0%	FINE SILT:	0.2%
V FINE GRAVEL:	0.0%	V FINE SILT:	0.2%
V COARSE SAND:	0.1%	CLAY:	0.2%

	METHOD OF MOMENTS			FOLK & WARD METHOD		
	Arithmetic μm	Geometric μm	Logarithmic ϕ	Geometric μm	Logarithmic ϕ	Description
MEAN ($\bar{x}$):	206.8	173.0	2.531	175.4	2.511	Fine Sand
SORTING (σ):	122.4	1.683	0.751	1.496	0.581	Moderately Well Sorted
SKEWNESS (Sk):	4.043	-2.102	2.102	0.014	-0.014	Symmetrical
KURTOSIS (K):	25.91	19.30	19.30	1.558	1.558	Very Leptokurtic

GRAIN SIZE DISTRIBUTION

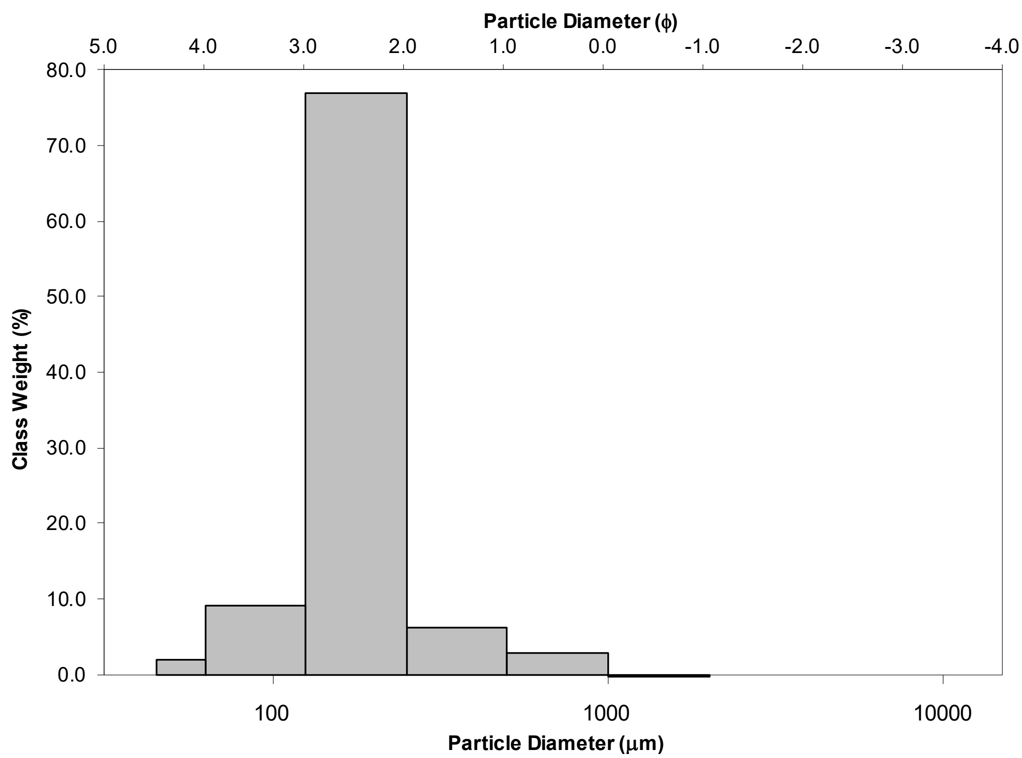

SAMPLE STATISTICS

SIEVING ERROR: 0.0%

SAMPLE IDENTITY: **BE_52** ANALYST & DATE: Leila Rashid, 28/10/2022

SAMPLE TYPE: Unimodal, Poorly Sorted TEXTURAL GROUP: Slightly Gravelly Sand

SEDIMENT NAME: Slightly Very Fine Gravelly Fine Sand

	μm	φ
MODE 1:	187.5	2.500
MODE 2:		
MODE 3:		
D_{10}:	66.19	0.843
MEDIAN or D_{50}:	226.6	2.142
D_{90}:	557.4	3.917
(D_{90} / D_{10}):	8.421	4.645
(D_{90} - D_{10}):	491.2	3.074
(D_{75} / D_{25}):	2.680	2.012
(D_{75} - D_{25}):	236.7	1.422

GRAIN SIZE DISTRIBUTION

GRAVEL:	0.2%	COARSE SAND:	9.7%
SAND:	90.6%	MEDIUM SAND:	33.3%
MUD:	9.3%	FINE SAND:	36.5%
		V FINE SAND:	9.4%
V COARSE GRAVEL:	0.0%	V COARSE SILT:	3.2%
COARSE GRAVEL:	0.0%	COARSE SILT:	1.2%
MEDIUM GRAVEL:	0.0%	MEDIUM SILT:	1.2%
FINE GRAVEL:	0.0%	FINE SILT:	1.2%
V FINE GRAVEL:	0.2%	V FINE SILT:	1.2%
V COARSE SAND:	1.7%	CLAY:	1.2%

	METHOD OF MOMENTS			FOLK & WARD METHOD		
	Arithmetic μm	Geometric μm	Logarithmic φ	Geometric μm	Logarithmic φ	Description
MEAN ($\bar{x}$):	307.7	193.1	2.373	219.7	2.187	Fine Sand
SORTING (σ):	270.1	3.028	1.599	2.464	1.301	Poorly Sorted
SKEWNESS (Sk):	3.355	-1.632	1.632	-0.171	0.171	Fine Skewed
KURTOSIS (K):	23.87	6.260	6.260	1.453	1.453	Leptokurtic

GRAIN SIZE DISTRIBUTION

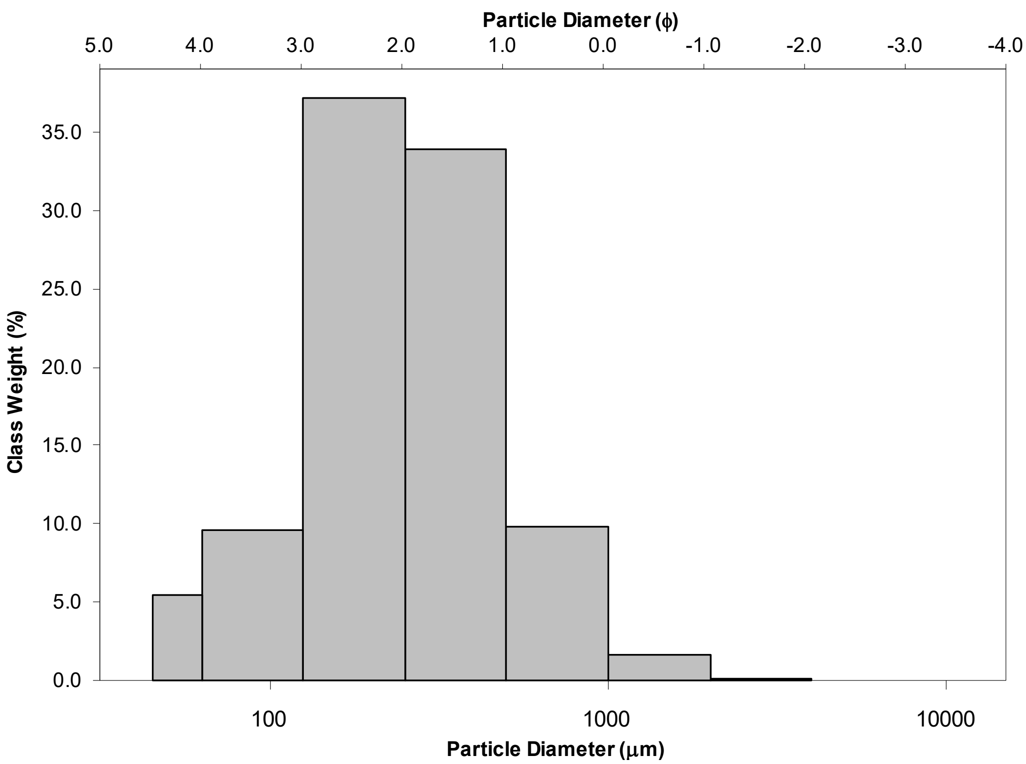

SIEVING ERROR: 4.1%

SAMPLE STATISTICS

SAMPLE IDENTITY: **BW_51** ANALYST & DATE: Leila Rashid, 28/10/2022

SAMPLE TYPE: Unimodal, Poorly Sorted TEXTURAL GROUP: Muddy Sand

SEDIMENT NAME: Very Coarse Silty Fine Sand

	μm	ϕ
MODE 1:	187.5	2.500
MODE 2:		
MODE 3:		
D_{10}:	50.33	1.335
MEDIAN or D_{50}:	156.8	2.673
D_{90}:	396.5	4.312
(D_{90} / D_{10}):	7.877	3.231
$(D_{90} - D_{10})$:	346.1	2.978
(D_{75} / D_{25}):	2.566	1.648
$(D_{75} - D_{25})$:	142.5	1.360

GRAIN SIZE DISTRIBUTION

GRAVEL:	0.0%	COARSE SAND:	3.9%
SAND:	87.6%	MEDIUM SAND:	16.1%
MUD:	12.4%	FINE SAND:	43.5%
		V FINE SAND:	23.4%
V COARSE GRAVEL:	0.0%	V COARSE SILT:	4.5%
COARSE GRAVEL:	0.0%	COARSE SILT:	1.6%
MEDIUM GRAVEL:	0.0%	MEDIUM SILT:	1.6%
FINE GRAVEL:	0.0%	FINE SILT:	1.6%
V FINE GRAVEL:	0.0%	V FINE SILT:	1.6%
V COARSE SAND:	0.7%	CLAY:	1.6%

	METHOD OF MOMENTS			FOLK & WARD METHOD		
	Arithmetic μm	Geometric μm	Logarithmic ϕ	Geometric μm	Logarithmic ϕ	Description
MEAN ($\bar{x}$):	207.6	129.3	2.951	149.7	2.740	Fine Sand
SORTING (σ):	186.2	2.982	1.576	2.437	1.285	Poorly Sorted
SKEWNESS (Sk):	3.247	-1.435	1.435	-0.215	0.215	Fine Skewed
KURTOSIS (K):	19.19	5.314	5.314	1.496	1.496	Leptokurtic

GRAIN SIZE DISTRIBUTION

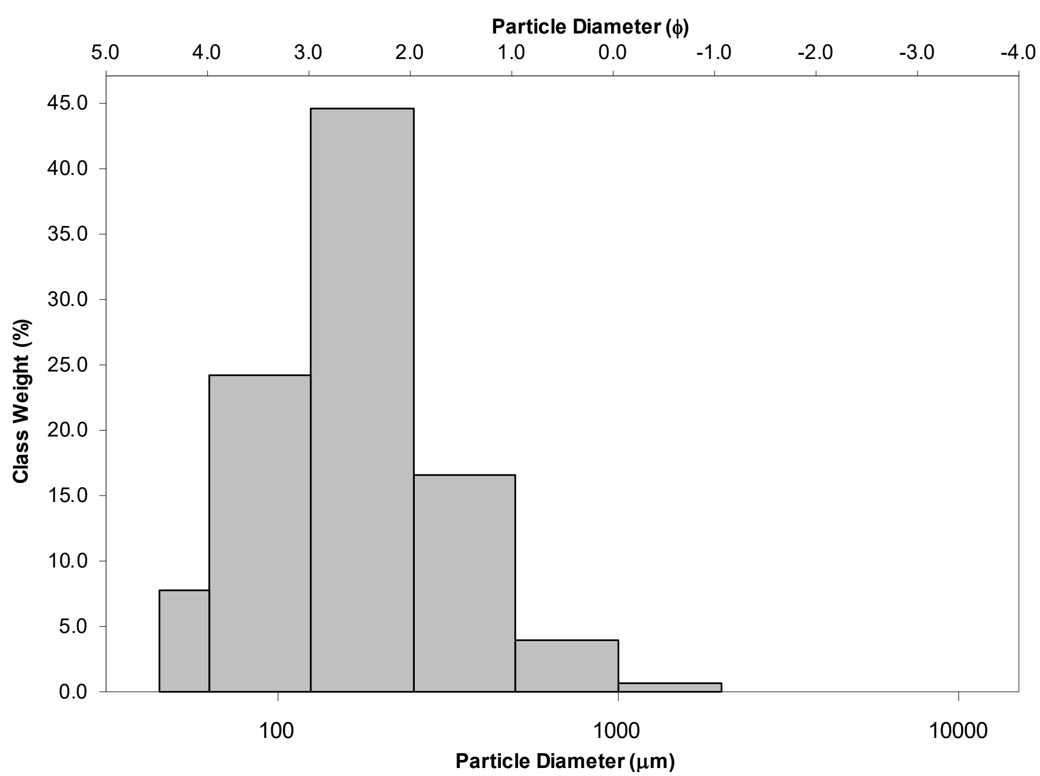

SIEVING ERROR: 0.0%

SAMPLE STATISTICS

SAMPLE IDENTITY: **BW_53** ANALYST & DATE: Leila Rashid, 28/10/2022

SAMPLE TYPE: Unimodal, Moderately Sorted TEXTURAL GROUP: Slightly Gravelly Sand

SEDIMENT NAME: Slightly Very Fine Gravelly Fine Sand

	μm	ϕ
MODE 1:	187.5	2.500
MODE 2:		
MODE 3:		
D_{10}:	109.0	1.300
MEDIAN or D_{50}:	182.2	2.456
D_{90}:	406.0	3.197
(D_{90} / D_{10}):	3.724	2.459
(D_{90} - D_{10}):	297.0	1.897
(D_{75} / D_{25}):	1.638	1.339
(D_{75} - D_{25}):	90.77	0.712

GRAIN SIZE DISTRIBUTION

GRAVEL:	0.4%	COARSE SAND:	5.2%
SAND:	96.9%	MEDIUM SAND:	11.3%
MUD:	2.7%	FINE SAND:	70.3%
		V FINE SAND:	9.1%
V COARSE GRAVEL:	0.0%	V COARSE SILT:	1.2%
COARSE GRAVEL:	0.0%	COARSE SILT:	0.3%
MEDIUM GRAVEL:	0.0%	MEDIUM SILT:	0.3%
FINE GRAVEL:	0.0%	FINE SILT:	0.3%
V FINE GRAVEL:	0.4%	V FINE SILT:	0.3%
V COARSE SAND:	1.0%	CLAY:	0.3%

	METHOD OF MOMENTS			FOLK & WARD METHOD		
	Arithmetic μm	Geometric μm	Logarithmic ϕ	Geometric μm	Logarithmic ϕ	Description
MEAN ($\bar{x}$):	250.2	186.3	2.424	188.3	2.409	Fine Sand
SORTING (σ):	261.2	1.979	0.985	1.670	0.740	Moderately Sorted
SKEWNESS (Sk):	6.282	-1.130	1.130	0.143	-0.143	Coarse Skewed
KURTOSIS (K):	56.93	12.48	12.48	1.758	1.758	Very Leptokurtic

GRAIN SIZE DISTRIBUTION

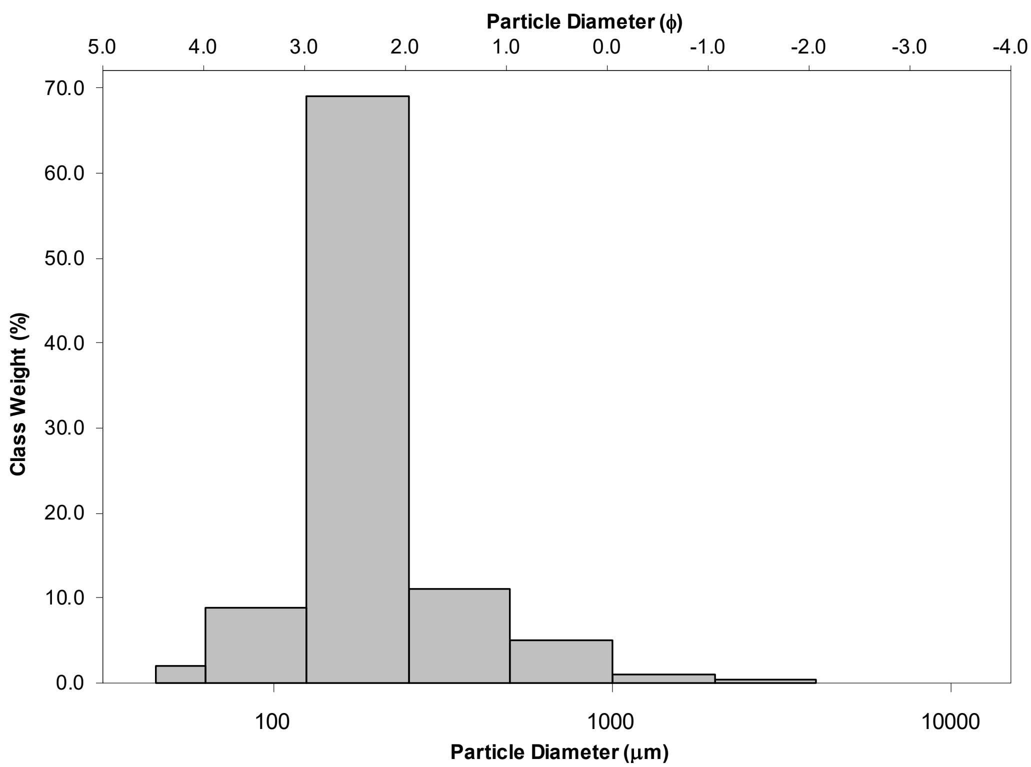

SAMPLE STATISTICS

SIEVING ERROR: 0.0%

SAMPLE IDENTITY: **BW_54**

ANALYST & DATE: Leila Rashid, 28/10/2022

SAMPLE TYPE: Unimodal, Moderately Well Sorted

TEXTURAL GROUP: Slightly Gravelly Sand

SEDIMENT NAME: Slightly Very Fine Gravelly Fine Sand

	μm	ϕ
MODE 1:	187.5	2.500
MODE 2:		
MODE 3:		
D_{10}:	103.2	2.053
MEDIAN or D_{50}:	171.0	2.548
D_{90}:	241.0	3.276
(D_{90} / D_{10}):	2.334	1.596
$(D_{90} - D_{10})$:	137.8	1.223
(D_{75} / D_{25}):	1.535	1.276
$(D_{75} - D_{25})$:	73.87	0.618

GRAIN SIZE DISTRIBUTION

GRAVEL:	1.7%	COARSE SAND:	0.9%
SAND:	97.1%	MEDIUM SAND:	2.2%
MUD:	1.2%	FINE SAND:	80.9%
		V FINE SAND:	12.2%
V COARSE GRAVEL:	0.0%	V COARSE SILT:	0.6%
COARSE GRAVEL:	0.0%	COARSE SILT:	0.1%
MEDIUM GRAVEL:	0.0%	MEDIUM SILT:	0.1%
FINE GRAVEL:	0.8%	FINE SILT:	0.1%
V FINE GRAVEL:	0.9%	V FINE SILT:	0.1%
V COARSE SAND:	1.0%	CLAY:	0.1%

	METHOD OF MOMENTS			FOLK & WARD METHOD		
	Arithmetic μm	Geometric μm	Logarithmic ϕ	Geometric μm	Logarithmic ϕ	Description
MEAN ($\bar{x}$):	259.5	174.3	2.520	171.0	2.548	Fine Sand
SORTING (σ):	525.5	1.825	0.868	1.428	0.514	Moderately Well Sorted
SKEWNESS (Sk):	7.557	1.502	-1.502	-0.064	0.064	Symmetrical
KURTOSIS (K):	64.11	19.42	19.42	1.331	1.331	Leptokurtic

GRAIN SIZE DISTRIBUTION